PNL-4774
1

NUREG/CR-3384
PNL-4774

VISA - A Computer Code for Predicting the Probability of Reactor Pressure Vessel Failure

Prepared by D. L. Stevens, F. A. Simonen, J. Strosnider, Jr.,
R. W. Klecker, D. W. Engel, K. I. Johnson

Pacific Northwest Laboratory
Operated by
Battelle Memorial Institute

Prepared for
U.S. Nuclear Regulatory Commission

GPO Printed copy price: $4.50

NUREG/CR-3384
PNL-4774
AM

VISA - A Computer Code for Predicting the Probability of Reactor Pressure Vessel Failure

Manuscript Completed: July 1983
Date Published: September 1983

Prepared by
D. L. Stevens, F. A. Simonen, J. Strosnider, Jr.*,
R. W. Klecker*, D. W. Engel, K. I. Johnson

Pacific Northwest Laboratory
Richland, WA 99352

*U. S. Nuclear Regulatory Commission

Prepared for
Division of Engineering Technology
Office of Nuclear Regulatory Research
U.S. Nuclear Regulatory Commission
Washington, D.C. 20555
NRC FIN B2310

ABSTRACT

The VISA (Vessel Integrity Simulation Analysis) code was developed as part of the NRC staff evaluation of pressurized thermal shock. VISA uses Monte Carlo simulation to evaluate the failure probability of a pressurized water reactor (PWR) pressure vessel subjected to a pressure and thermal transient specified by the user. Linear elastic fracture mechanics are used to model crack initiation and propagation. Parameters for initial crack size, copper content, initial RT_{NDT}, fluence, crack-initiation fracture toughness, and arrest fracture toughness are treated as random variables. This report documents the version of VISA used in the NRC staff report (Policy Issue from J. W. Dircks to NRC Commissioners, "Enclosure A: NRC Staff Evaluation of Pressurized Thermal Shock, November 1982," SECY-82-465) and includes a user's guide for the code.

CONTENTS

VISA, A COMPUTER CODE FOR PREDICTING THE PROBABILITY OF REACTOR VESSEL FAILURE RESULTING FROM PRESSURIZED THERMAL SHOCK

1.0 INTRODUCTION

The VISA code was developed by NRC staff members to analyze, through simulation, the integrity of a nuclear reactor pressure vessel. The code was used by NRC staff members to facilitate evaluation of pressurized thermal shock (PTS) in reactor pressure vessels (RPVs).

The code is divided into two sections. The first section, discussed in Chapter 2, performs a deterministic fracture mechanics analysis for a user-defined temperature and pressure transient. The analysis yields values of the stress intensity factors and temperatures at 32 depths through the wall and for ten times measured from the start of the transient. These values are stored for use in the second section of the code.

The second section of the code, discussed in Chapter 3, performs a Monte Carlo analysis of the probability of vessel failure. Flaw depth and vessel toughness are treated as random. Sampled values of vessel toughness are compared to the stored values of the stress intensity factor at a sampled flaw depth to determine crack initiation or growth. The proportion of vessel failures in a large number of trial comparisons is an estimate of the probability of vessel failure.

1.1 BACKGROUND

Reactor pressure vessels have long been considered extremely reliable components of pressurized water reactors (PWRs). There have been relatively few disruptive failures (loss of the pressure-retaining boundary) in non-nuclear pressure vessels, and no failures of nuclear RPVs. The disruptive failure rate has been estimated to be less than 10^{-6} per vessel year (Refs. 1, 2) for RPVs designed, fabricated, inspected, and operated in accordance with the Boiler and Pressure Vessel Code of the American Society of Mechanical Engineers (Ref. 3). Recent operating experience and results of surveillance and research programs, however, suggest the need to re-evaluate the probability of RPV failure.

Thermal hydraulic transients resulting in steep thermal gradients and thermal stresses across the vessel wall can occur in PWRs. If, simultaneously, the vessel is pressurized (or repressurized during the transient), the pressure stress is superimposed on the thermal stress, resulting in what is known as a pressurized thermal shock transient. Both the pressure and thermal stresses are tensile stresses and tend to open cracks located on the inner surface of the vessel. Eight significant PTS transients have occurred since 1970 (Ref. 4).

Pressurized thermal shock events are of concern only for older PWRs. New pressure vessels have a relatively high fracture toughness, which is gradually degraded by neutron irradiation. The presence of certain trace elements, notably copper, in the vessel's weld material increases the rate of degradation. If the fracture toughness has been sufficiently reduced, a severe PTS event could cause propagation of small flaws that might exist near the inner surface of the vessel.

The NRC staff evaluated PTS in the spring of 1981 and concluded that no immediate licensing actions were needed to ensure short-term vessel integrity; however, further, extensive studies were deemed necessary to determine whether or not and when corrective actions would be needed to ensure vessel integrity throughout the intended service life of the vessel. Specifically, the NRC staff wanted a more precise method of quantifying the probability of vessel failure due to PTS. The VISA (Vessel Integrity Simulation Analysis) computer code was developed as a part of the effort to meet this need.

This report documents the version of the VISA code used by the NRC staff to evaluate PTS (Ref. 4) and contains a user's guide for the VISA code.

The evaluation of PTS is not complete, nor does the VISA code described in this report represent a finished product. Research sponsored by NRC and industry is underway to provide a better understanding of event sequences leading to PTS, and to obtain additional information on vessel toughness, fluence effects, weld chemistry, and flaw-size distributions. Scientists at Pacific Northwest Laboratory (PNL) are evaluating the stochastic structure of the VISA code and plan to make some improvements in the code. As the work is completed, updated versions of this report will be issued.

1.2 GENERAL DESCRIPTION OF THE VISA CODE

Estimates of failure probabilities can be obtained by analyzing observed failures or by modeling mathematically the failure process. The mathematical model approach was adopted in VISA because no RPVs have actually failed, and because a model allows the uncertainties in various properties that affect the failure process to be evaluated. The failure process is assumed to result from pre-existent flaws in the weld material of the pressure vessel; therefore, fracture-mechanics relationships are the bases for the mathematical model. Only welds are evaluated in the model because they have greater likelihood for flaws and are more sensitive than the base material to damage from radiation. Thus, weld behavior should dominate the failure probability.

VISA is a simulation model, which means that failure probability is assessed by performing a large number of deterministic evaluations with random values selected for various parameters. The fracture mechanics analysis is described in Chapter 2, and the simulation model is described in Chapter 3.

A typical RPV is fabricated with either a ring-forging beltline shell or a rolled and welded beltline shell (Figure 1.1). The rolled and welded beltline configuration has six longitudinally oriented beltline welds. The failure probability of longitudinally or circumferentially oriented welds can be evaluated by using the appropriate flaw size distribution. The current version of VISA, presented in this report, calculates the failure probability for a single, longitudinally oriented beltline weld. The total probability of failure can be obtained by combining the probability from each of the welds. (If the weld failures are independent and the failure probabilities are small, the total failure probability is simply the sum of the individual failure probabilities for each weld. Otherwise, intersection probabilities must be considered.)

The VISA code evaluates the conditional probability of RPV failure given a specified thermal and pressure transient. The user can specify the thermal transient with either a polynomial representation or an exponential decay model. The pressure transient is specified with a polynomial. The probability of vessel failure can be obtained by multiplying the conditional probability from VISA by the probability of the transient.

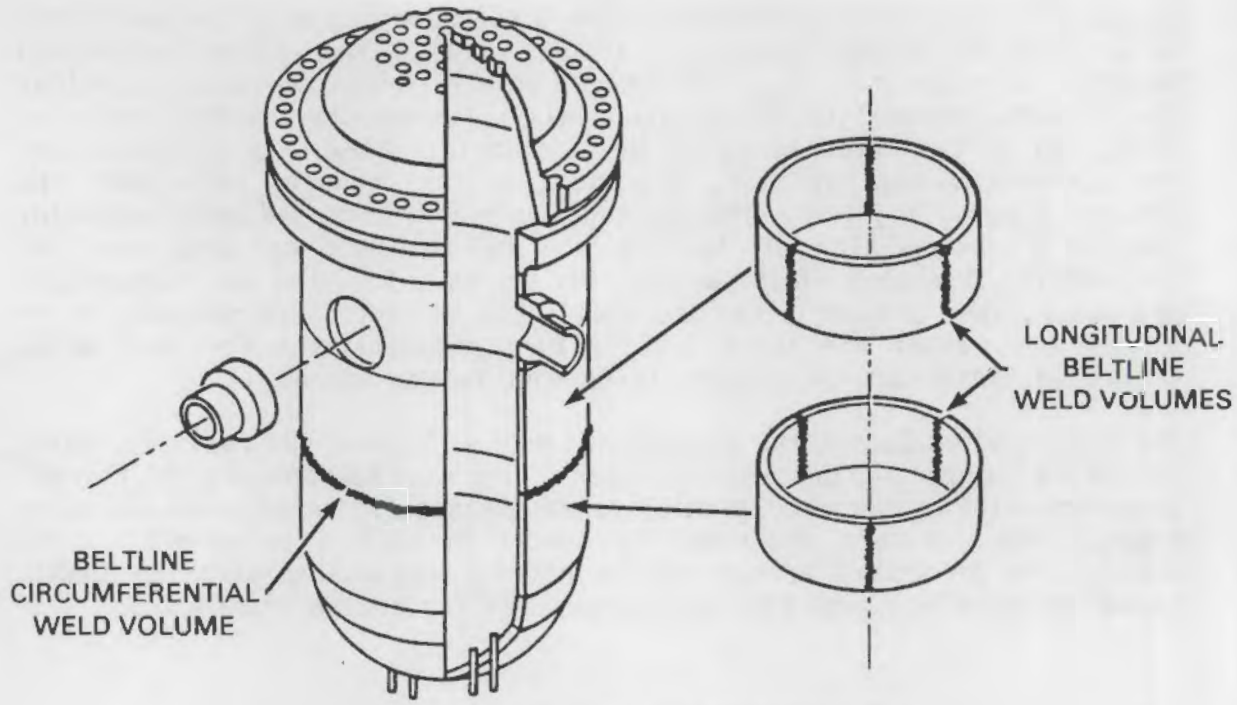

1(a) ROLLED AND WELDED BELTLINE SHELL

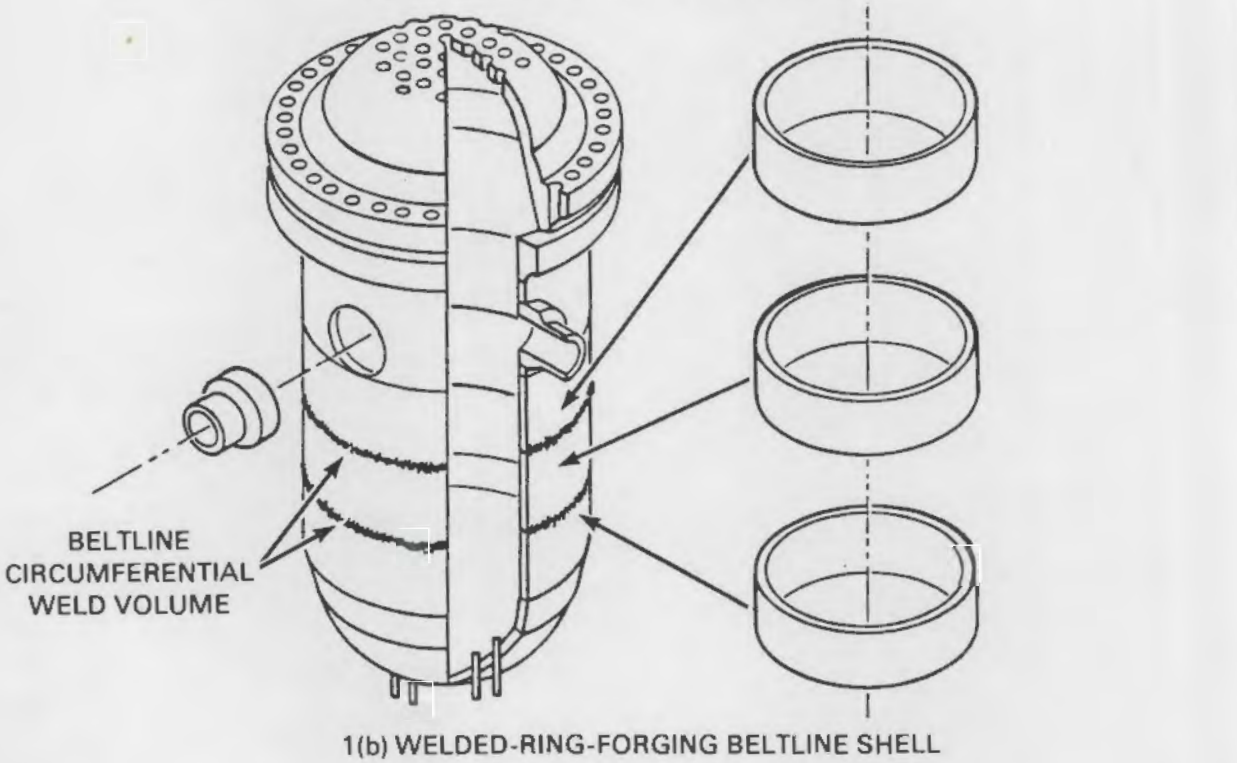

1(b) WELDED-RING-FORGING BELTLINE SHELL

FIGURE 1.1. Fabrication Configurations of PWR Beltline Shells (from Ref. 4)

2.0 DETERMINISTIC FRACTURE MECHANICS ANALYSIS

The first part of the VISA code is a deterministic fracture mechanics analysis. In this report, "fracture mechanics analysis" includes heat transfer and stress analyses as well as the calculation of crack-tip stress intensity factors. This analysis provides input to the subsequent Monte Carlo assessment of vessel failure probability, which is based on a large number of deterministic calculations with variation of the parameters of flaw size and vessel toughness. With appropriate interfaces, the probabilistic portion of the VISA code can also be used as a post-processor to other deterministic analysis codes.

2.1 OVERVIEW OF DETERMINISTIC ANALYSIS

VISA uses closed-form solutions for heat transfer and stress calculations. These derivations were developed by NRC in 1978 and are presented in Appendix A of this report. Applied stress intensity factors are calculated in VISA using influence coefficients developed by Heliot, Labbens and Pellissier-Tanon using linear elastic boundary integral methods (Refs. 5, 6). These influence coefficients were developed for RPVs with a radius to wall-thickness ratio of ten, and this R/t ratio is assumed in the VISA code.

The inputs for the deterministic calculations include 1) pressure and temperature of the reactor coolant as a function of time for a given transient, 2) surface heat transfer coefficient, 3) material properties, 4) fluence at the inside surface of the vessel, and 5) wall thickness of the vessel. The code performs heat transfer, stress analysis, and fracture mechanics calculations. Output from the deterministic analyses is summarized as values of crack-tip stress intensity factors and the corresponding values of crack-tip temperatures, initiation toughness, and arrest toughness. These parameters are calculated for 32 values of crack depth and for ten values of time. All temperature and stress data are referenced to a radial coordinate measured from the interface between the base metal of the ferritic vessel and the stainless steel clad layer.

A flow chart summarizing the deterministic portion of the fracture mechanics analysis is given in Figure 2.1. The first block on the flow chart involves input for both the deterministic and probabilistic portions of the VISA code. Probabilistic inputs are set aside during the deterministic calculation but are later available for use in the probabilistic portion of the VISA calculation.

The user has the option of performing only the deterministic calculation, without going on to the probabilistic evaluation of vessel failure. Used in this manner, the VISA code is similar to the OCA-I code developed at Oak Ridge National Laboratory for deterministic fracture mechanics analyses of vessels under conditions of pressurized thermal shock (Ref. 7). However, the numerical methods used by OCA-I and VISA differ in several significant respects, and OCA-I is, in general, a superior code for deterministic (as opposed to probabilistic) PTS analyses.

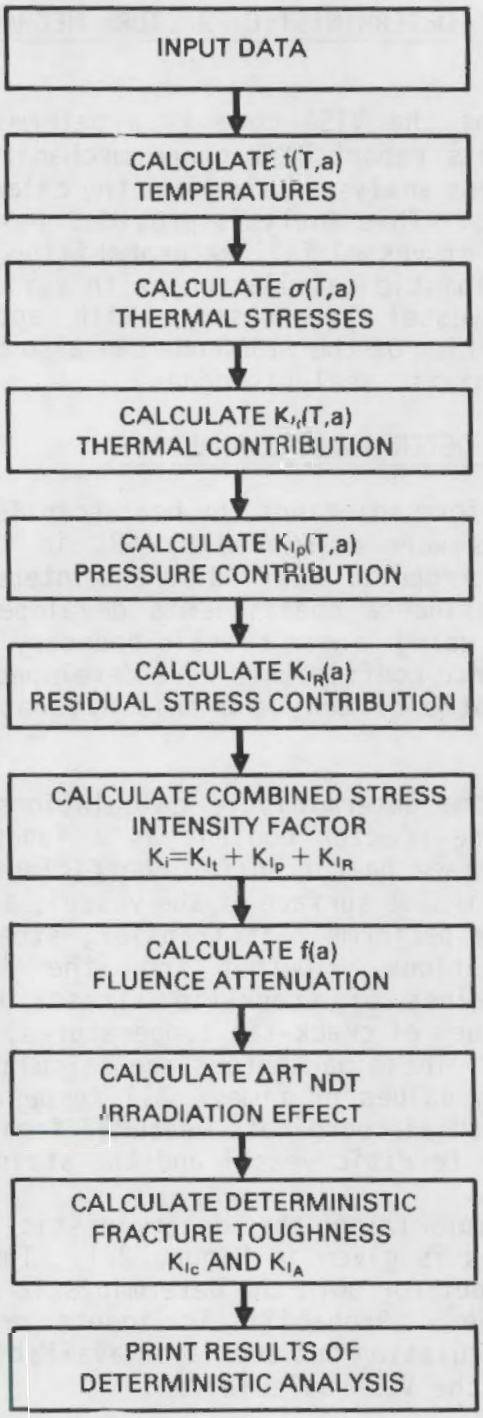

FIGURE 2.1. Flow Chart for Deterministic Fracture Mechanics Analysis

2.2 HEAT TRANSFER

Details of the closed-form solution used to calculate temperature distributions across the vessel wall versus time are provided in Appendix A. For the heat transfer calculation, a slab geometry is assumed, and in the one-dimensional solution, heat flow occurs only through the wall. For typical reactor vessels with a radius to wall-thickness ratio of ten or more, the error introduced by this assumption is negligible compared to other uncertainties in the analysis. The slab geometry is also used for thermal stress analyses, but a cylindrical geometry is used to analyze the stress from pressure and to calculate stress intensity factors.

2.2.1 Heat Transfer Coefficient

The VISA code treats the heat transfer coefficient, h, as constant with time. Also, the one-dimensional analysis implies an assumption that h is the same for all water-cooled portions of the vessel wall.

The simplified assumptions in VISA neglect the fact that during a typical transient, h can vary over a considerable range, depending on the hydraulic and thermal conditions. The value of h as a function of time can be difficult to determine because of hydraulic and other uncertainties. Therefore, when using the VISA code, it is recommended that conservative values of h be selected. In this regard, for values of heat transfer coefficients in the range of interest for most thermal transients (approximately 300 BTU/hr ft^2 ^oF), short perturbations to higher values do not cause significant increases in thermal stress.

The heat transfer coefficient, h, as utilized in the VISA code, should be modified to simulate the thermal effect of clad (Ref. 4), since the VISA heat transfer model does not explicitly include cladding. Thus, the value of h supplied as input to VISA should account for the fluid-to-surface heat transfer coefficient along with a contribution due to the thermal resistance of the clad. This effective value of heat transfer coefficient is determined from the following equation:

$$h_{eff} = \frac{1}{\frac{1}{h_f} + \frac{th}{k}} \tag{2.1}$$

where h_f is the fluid heat transfer coefficient in BTU/hr ft^2 ^oF, k is the thermal conductivity of the stainless steel clad in BTU/hr ft ^oF, and th is the thickness of the stainless steel cladding in inches.

The effective value of h is supplied as input to VISA in an indirect manner through the dimensionless parameter

$$C = \frac{(h_{eff})\ (th)}{k} \tag{2.2}$$

which is related to the transcendental equation $\alpha \tan \alpha = C$. The roots of this equation govern the temperature solutions (see Appendix A). In VISA, general values of C are not programmed, but rather five discrete values of C (6.0, 10.0, 20.0, 40.0 and 60.0) are selected. While some generality is lost, this range of values is sufficient to approximate the heat transfer conditions of interest in vessel transients.

2.2.2 Temperature Dependence of Thermal Diffusivity

The VISA code allows the user to assume either temperature-dependent or temperature-independent heat transfer characteristics for the vessel material. If temperature-dependent properties are desired, then the analyses use a set of predefined curves for the thermal diffusivity. The curves are used in an iterative manner; that is, the property values associated with the calculated temperature are compared to the value from the previous iteration, and the process continues until the values agree within a small tolerance. The predefined curves (described in Appendix A) correspond to values from the ASME Boiler and Pressure Vessel Code.

The user can specify a value of thermal diffusivity to evaluate a vessel made of a material that differs from the default option in the VISA code. In this case, the heat transfer properties are not treated as temperature dependent. Therefore, the user must specify a representative value of diffusivity for the metal temperatures expected during the transient of interest.

2.2.3 Specification of Transient

Prior to the thermal transient, the vessel wall is assumed to be at a uniform temperature, and this temperature is used as input to VISA. During the transient, heat flow at the outer, insulated surface of the vessel is assumed to be zero. The vessel is cooled or heated at the inner surface only -- no sources of heat exist within the metal. The specified value of the uniform, initial temperature of the vessel will normally correspond to the specified coolant temperature at time equals zero. However, VISA does permit a step change in temperature to be specified at time zero.

The VISA code does not treat histories of coolant temperature and pressure that are completely general or arbitrary. Rather, the closed-form solutions use polynomial and exponential functions that can approximate a wide range of transients.

The exponential temperature has the form

$$T = T_o + (T_f - T_o)\,(1 - e^{-\beta t}) \qquad (2.3)$$

where

T = temperature of coolant, ^{o}F

T_o = initial coolant temperature, ^{o}F

T_f = final coolant temperature, ^{o}F

β = decay constant, min^{-1}

t = time, min.

The user must specify the parameters T_o, ΔT and β that best describe the transient of interest. The change in temperature ($\Delta T = T_f - T_o$) must have a minus sign if the temperature decreases.

The user also can select a fourth-order polynomial approximation of the coolant temperature, rather than selecting an exponential approximation. Five time-temperature pairs, beginning at time zero and continuing at equal intervals in time, are supplied as input to VISA; the polynomial fit is performed by VISA. For complex thermal transients, the user must select the time values carefully to ensure that the fitted polynomial does not significantly differ from the desired temperature transient between the fitted points.

The time history of the pressure is described by a fourth-order polynomial in a fashion similar to the thermal history. No exponential or other form of approximation can be used in place of the fourth-order polynomial.

2.2.4 Effect of Cladding

The VISA code assumes that a given vessel wall is made of only one type of material, and does not directly treat heat transfer through the clad material. However, the thermal effect of clad can be treated by modifying the coefficient of surface heat transfer (see Section 2.2.1). The procedure is illustrated in the verification calculations described in Appendix B.

2.2.5 Series Solution

Metal temperature distributions at various times during a transient are based on infinite-series solutions. Details of the solutions are described in Appendix A. Four terms of the series are used in the analysis. The error introduced by limiting the number of terms is significant only at or very shortly after the start of the transient (time = zero) where an infinite number of terms is required to obtain correct temperatures. Shortly thereafter, higher terms in the series decay rapidly to insignificant values. For the transients of interest, the crack initiation generally occurs relatively late in the transient, and if it occurs, little error is introduced by using a finite number of terms.

2.3 STRESS ANALYSIS

Series solutions are used in VISA to calculate thermal stress distributions through the vessel wall. Pressure stresses are calculated using solutions from elasticity theory for thick-walled cylinders. Details of these solutions are given in Appendix A.

2.3.1 Elastic Behavior

The deterministic stress analysis in VISA assumes linear elastic material behavior. This implies that the total peak stresses (thermal plus pressure plus residual plus any other stresses) are less than, or at least not significantly greater than, the yield strength of the material. Under these assumptions, components of stress can be added, and procedures of linear-elastic fracture mechanics can be used. For rapid thermal transients, high stresses usually occur locally at the inside surface of the vessel wall, and acceptable stress distributions (total stress below yield) over the remaining section can still be obtained if the overstressed region is relatively thin.

2.3.2 Temperature Dependence of $E\alpha/(1-\nu)$

The VISA code provides two options on the material properties, where α is the thermal expansion coefficient, E is the elastic modulus, and ν is the Poisson's ratio. In the first option, temperature-dependent properties can be selected, but the analyses use a predefined curve for $E\alpha/(1-\nu)$. These properties, described in Appendix A, are typical properties for reactor vessel steels as given by the ASME Boiler and Pressure Vessel Code.

As a second option, the user may specify a constant value for $E\alpha/(1-\nu)$. This value is not treated as temperature dependent, and must be carefully selected to be representative of the metal temperatures during the transient of interest. Particular attention must be given to the value of the expansion coefficient. Thermal expansion curves show noticeable nonlinearity in the range from room temperature to reactor operating temperatures. It is important to use an expansion coefficient corresponding to the mean slope of the expansion curve for the expected metal temperatures.

2.3.3 Effect of Cladding

The version of the VISA code described in this report does not account for the stresses induced by differences in thermal expansion between the stainless steel of the cladding and the ferritic steel of the vessel wall. The vessel wall is assumed to be of a single material.

The effects of clad on vessel stresses are discussed in an NRC staff report (Ref. 4). Results of calculations performed outside the scope of the VISA code are also described. Because material and physical properties of the stainless steel cladding differ from those of the carbon steel wall, the cladding effect can be a factor in analyses of vessel integrity. The stress effect of the clad, however, depends on the stress relief and operational history of the vessel. Once clad stresses are established, the

effect of clad stress can be accommodated by superposition of cladding-induced stresses with those of other causes.

2.3.4 Residual Stresses

The VISA code does not account for residual stresses in the welds of vessels. While the code is structured to treat such stresses, additional development of the code would be required to activate this logic in the stress and fracture mechanics calculations.

2.3.5 Series Solution

Thermal stresses are computed using the infinite-series solution, which is discussed in detail in Appendix A. As with the temperature solution, the evaluation of the series in VISA is truncated after the fourth-order terms.

2.4 FRACTURE MECHANICS ANALYSIS

The VISA code is based on linear elastic fracture mechanics and uses influence coefficients developed by Heliot, Labbens and Pellissier-Tanon (Refs. 5, 6) to calculate crack-tip stress intensity factors. The flaws are assumed to be infinitely long surface cracks extending from the inside surface of the vessel.

2.4.1 Stress Intensity Factors

At each time step, thermal and other stresses are expressed as polynomial functions of the relative depth of the location of interest into the wall of the vessel:

$$\sigma\left(\frac{X}{L}, t\right) = \sum_{j=0}^{4} \sigma_j \left(\frac{X}{L}\right)^j \qquad (2.4)$$

where σ_j's are constants determined by curve fitting. The stress intensity factor for this stress distribution is then

$$K_I = \sqrt{\pi a} \sum_{j=0}^{4} \sigma_j \left(\frac{a}{L}\right)^j i_j \quad . \qquad (2.5)$$

In the VISA code, the influence functions (i_j) are expressed as polynomial functions of the relative depth of the crack. Different expressions for the i_j's can be used for different crack geometries and directions. Both "long" axial flaws (two dimensional) and continuous 360° circumferential flaws are treated by VISA. Influence functions have also been calculated by Heliot, Labbens and Pellissier-Tanon for elliptical flaws with an aspect ratio of 1 to 3. These influence functions are presented in Appendix A.

The influence functions apply specifically to a vessel that has a ratio of wall thickness to radius equal to 1:10. This ratio approximates the geometry for most vessels in pressurized water reactors. Errors from the

use of the 1:10 ratio should be relatively insignificant compared to errors resulting from the many uncertainties in other inputs to the analyses of vessel failure probability.

Plastic fracture considerations do not enter into the deterministic portion of the VISA code. However, the predictions of vessel failure probability in the subsequent Monte Carlo analyses does address vessel failure due to plastic collapse of the net-section. The net-section stress of arrested cracks is compared to the specified value of flaw stress for the irradiated material, and vessel failure is predicted when the flow stress is exceeded.

2.4.2 Fracture Mechanics Output

The deterministic analysis gives a table of stress intensity factors for a total of 32 crack depths ranging from a minimum depth of 0.125 in. to a maximum depth of 7.75 in. The table of stress intensity factors is constructed for a total of ten equal time steps during the transient.

The printed output of the deterministic analysis also includes values of temperature, initiation toughness, and arrest toughness. All values are evaluated for the crack depth and time corresponding to the stress intensity factors. The fracture toughness values in the output tables of the deterministic analysis are based on user input values of copper content, fluence, and initial RT_{NDT}. For the deterministic analysis, the radiation-induced shift in RT_{NDT} is calculated using equations in Regulatory Guide 1.99 (Ref. 8). The attenuation of fluence through the vessel wall is based on an exponential model using the equation

$$f = f_0 \, e^{-0.33x} \qquad (2.6)$$

where f_0 is the fluence at the inside surface and x is the depth measured in inches. Toughness versus temperature is from the reference curves of Section XI of the ASME Boiler and Pressure Vessel Code with a limit of 200 ksi $\sqrt{\text{in.}}$ on upper-shelf toughness. These deterministic values of toughness are not used in the subsequent probabilistic analyses. Rather, the toughness values are calculated by sampling distributions as part of the Monte Carlo analysis. The distributions used in the probabilistic analyses are described in Chapter 3 of this report, and are not based on the particular sets of curves in ASME Section XI and Regulatory Guide 1.99.

Separate tables of output are printed for axial cracks and for circumferential cracks. The VISA results for axial cracks correspond to an infinite flaw of a two-dimensional analysis. The circumferential flaw treated by VISA is a continuous 360 degree crack extending into the wall from the inside surface of the vessel. The subsequent probabilistic portion of the code calculates failure probabilities for either axial flaws or for circumferential flaws, as directed by input from the user.

2.4.3 Warm Prestress

The deterministic portion of the VISA code does not involve any consideration of warm prestress (WPS). Nevertheless, evaluation of effects of warm prestressing can be performed by examining the tabulated output values of the applied stress intensity factors. In the subsequent probabilistic calculations, the user can choose to include warm prestress in predicting vessel fracture. This is accomplished by checking the applied stress intensity value at the current time step to that in the previous time step and not allowing crack initiation if the applied stress intensity is decreasing as a function of time. No credit is given for potentially increased toughness of the material following an initial peak in the applied stress intensity factor (i.e., if K_I reaches a maximum, decreases, and then begins to increase again, WPS will only be effective during the time when K_I is decreasing. When the K_I value is increasing, crack initiation will be predicted when $K_I = K_{Ic}$.)

The reader is directed to Reference 4 for a detailed discussion of the theoretical basis and experimental data that support the concept of warm prestressing. It is sufficient for this report to state that initiation of crack propagation during temperature reduction cannot occur while the crack tip stress intensity factor is constant or decreasing. The physical picture of warm prestress is one of blunting of the crack tip and development of favorable residual stresses.

3.0 SIMULATION MODEL

The VISA code consists of two parts. The first is a deterministic fracture mechanics analysis for a specified pressure and temperature transient. The mathematical algorithms are described in Chapter 2 and Appendix A. The results of the fracture mechanics analysis include applied stress intensity factors and crack-tip temperatures, which are put aside and stored for use in the second part of the code.

The second part of the code uses Monte Carlo techniques to assess the probability of a pressure vessel failure. Generally, Monte Carlo methods are used to determine the probability distribution of a function of random variables. This is accomplished by making a large number of deterministic evaluations of the function with a different set of sampled values of the random variables for each evaluation. The sample values are obtained by generating random numbers. The algorithm for generating random numbers is discussed in Appendix C.

For the present case, the "function" is the computer code that performs the deterministic crack initiation and growth calculation. For each iteration, simulated values of initial RT_{NDT}, fluence at the inner wall of the RPV, flaw size, and copper content are selected from their respective distributions. With these values fixed for the iteration, the code steps through the time history of the transient. For each time step, the applied stress intensity factor at the crack tip is taken from the stored values from the deterministic portion of the code. The fluence at the crack tip is calculated using Equation 2.6 and the sampled value of fluence at the inner wall of the RPV. The value of the shift in RT_{NDT} is calculated using the sampled copper value and the attenuated fluence. The value of the shift is then added to the sampled initial RT_{NDT} to obtain the adjusted RT_{NDT}. The value of fracture toughness, K_{Ic}, is sampled and compared to the stress intensity factor at the crack tip to determine crack initiation. The mean value of K_{Ic} is calculated using the adjusted RT_{NDT} and the temperature at the crack tip. The warm prestress option is checked at this point. If the option is requested, initiation will not take place if the stress intensity factor is decreasing. Otherwise, crack growth is initiated if K_{Ic} is less than the applied stress intensity factor. If initiation does not occur, the simulation moves to the next step. If initiation occurs, the crack is extended 1/4 in. and the crack arrest toughness (K_{Ia}) is simulated. The mean value of K_{Ia} is calculated using the values of RT_{NDT}, fluence, and temperature at the crack tip. If arrest occurs, the simulation moves to the next time step; if not, the crack is extended another 1/4 in. and a new value of K_{Ia} is simulated. This process continues until either the vessel fails or the duration of the transient is reached.

Each pass through the simulation loop represents a single computer calculation conducted to determine if RPV failure will occur. Up to a million passes through this loop can be made. Each calculation results in one of three outcomes: 1) no crack initiation, 2) crack initiation followed by arrest, or 3) pressure vessel failure. The probability of vessel failure is obtained by dividing the number of evaluations that

resulted in failure by the total number of evaluations that were made. This is the calculational equivalent to subjecting a population of up to a million operating reactor pressure vessels to the pressurized thermal shock transient of interest and then inferring the failure probability based on the number of observed failures.

The validity of relevance of the estimated probability of vessel failure depend on both the correctness of the fracture mechanics algorithm and the correctness of the probability distributions of the random variables. The probability distributions used in VISA are discussed below.

3.1 FLAW SIZE DISTRIBUTION

Of the random variables considered in VISA, the size of cracks in the weld material probably has the greatest uncertainty. The crack size distributions in the literature are based on the experience of RPV fabricators and nondestructive examinations. The experience of RPV fabricators, however, does not lead directly to a quantifiable flaw distribution, and the nondestructive examinations are of limited utility since the flaws of interest are those of unknown size that were not detected.

The flaw size distribution used in VISA is derived from the distribution given in Ref. 9, henceforth referred to as the OCTAVIA distribution. The OCTAVIA distribution was characterized as giving the probability P_S that the longest crack in the weld volume of the beltline region fell into a particular crack-size interval. The OCTAVIA distribution uses the following flaw size probabilities:

Flaw Size (S), inches	Crack-Size Interval	Probability (P_S)
0.125	0 - 0.1875	0.25
0.25	0.1875 - 0.375	0.125
0.5	0.375 - 0.75	0.025
1	0.75 - 1.5	0.0025
2	1.5 - 2.5	0.00025
3	2.5+	0.000025

The OCTAVIA flaw distribution was modified for use in VISA by interpolating some additional size intervals and adjusting for the difference in weld volume considered. The additional flaw sizes used in VISA are greater than one inch. The interpolation was accomplished by fitting a quadratic through the last three points of the logarithm of the complemented cumulative OCTAVIA distribution. The values obtained from evaluating the quadratic at the interval endpoints were rounded to obtain consistency with the OCTAVIA distribution.

The OCTAVIA distribution leaves some probability unassigned, since the probabilities (P_S) sum to only 0.402775. The remaining probability can be assigned to flaw sizes that are inconsequential. For convenience, the class of inconsequential flaws will be labeled as zero size, corresponding to a weld free of flaws. With this convention, the interpolated distribution for the total weld volume is given as

Flaw Size (S), inches	Flaw-Size Interval	Probability (P_S)
0	0	0.597225
0.125	0 - 0.1875	0.25
0.25	0.1875 - 0.375	0.125
0.5	0.375 - 0.75	0.025
1.0	0.75 - 1.25	0.0022
1.5	1.25 - 1.75	0.000425
2.0	1.75 - 2.25	0.0001
2.5	2.25 - 2.75	0.00003
3.0	2.75 - 3.25	0.000015
3.5	3.25+	0.000005

Since the VISA code considers only a single beltline weld, or about 1/6 of the weld volume considered in the list above, the P_S above must be adjusted. Let $F_T(s) = \Sigma P_S$, $S \leq s$, be the cumulative probability function for the longest flaw in the total weld volume, and let $F_1(s)$ be the corresponding function for a single weld. Since there are six welds in the total volume, $F_1(s) = [F_T(s)]^{1/6}$. Interval probabilities can be obtained by taking successive differences. The resulting flaw size distribution used in VISA is given by

Flaw Size (inches)	Probability
0	0.91767661
0.125	0.05507015
0.25	0.02256957
0.5	0.00422063
1.0	0.00036718
1.5	0.00007085
2.0	0.00001667
2.5	0.00000500
3.0	0.00000250
3.5	0.00000083

It should be noted that the flaw size distribution presented here and currently used in VISA is not exactly the same as was used in the NRC staff evaluation of PTS. That distribution was based on an incorrect interpolation of the OCTAVIA distribution. The error involved in the flaw size distribution used in the NRC staff report involved the probability of occurrence of relatively deep flaws which do not contribute significantly to the probability of the RPV failure under PTS conditions. Thus, the failure probabilities in the staff evaluation report were not affected significantly by the error.

Also, the efficiency of the code could be improved if small flaw sizes are considered non-failures, because the fracture mechanics calculations would not have to be performed. This method should be used only if the user is certain that small flaw sizes do not contribute significantly to the RPV failure probability. Future versions of the VISA code will include this as an input-controlled option.

3.2 COPPER CONTENT DISTRIBUTION

A truncated normal distribution is used for copper content, with a lower limit of 0.08 and an upper limit of 0.40. The mean and standard deviation of the distribution are set by the user. Limited data suggest that typical values for the mean copper content would be in the range of 0.2 to 0.3 weight percent, with a standard deviation in the range of 0.02 to 0.07 weight percent. For the analyses of specific vessels, mean copper contents can be estimated if data from chemical analyses of welds are available.

3.3 RT_{NDT} DISTRIBUTION

The distribution of the initial RT_{NDT} is dependent on both material variability and errors in the measurement process. Metallurgists at materials testing laboratories have indicated a belief in an accuracy of $\pm 20^{o}F$. Data presented by Combustion Engineering (Ref. 10) had a standard deviation of $17^{o}F$; however, these data were insufficient to properly characterize the distribution. The distribution assumed in VISA is a normal distribution with a standard deviation of $15^{o}F$. The mean value is an input quantity.

The shift in RT_{NDT} has been represented by the following equation:

$$\Delta RT_{NDT} = [-4.83 + 476 \cdot Cu + 267 \cdot Cu \cdot Ni]\,[F/10^{19}]^{0.218}$$

where

ΔRT_{NDT} = the shift in RT_{NDT}

Cu = the copper content in weight percent

Ni = the nickel content in weight percent

F = the fluence in neutrons (E > 1 MEV)/cm^2.

This equation was developed by George Guthrie at the Hanford Engineering Development Laboratory, Richland, Washington, through regression analysis of surveillance and research-program results. The effect of nickel has just recently been recognized and should be treated as a random variable. Although future versions of VISA will do so, the current version has a constant value of 0.65 percent for nickel content.

The value of RT_{NDT} is not treated as a random variable in VISA. It is believed that much of the variability of the observed values of ΔRT_{NDT} about the regression line was due to uncertainty in the measured values of fluence and copper content. Since the uncertainties in copper content and fluence are explicitly considered, it was considered inappropriate to include this variability twice. This point is being re-evaluated, and the approach may be changed in future versions of VISA.

3.4 NEUTRON FLUENCE DISTRIBUTION

The uncertainty in the fluence at the inner wall of the pressure vessel results from spatial variation of neutron spectra and flux as well as

computational inaccuracies. Current estimates indicate that the neutron fluence at the inner wall of the vessel can be predicted within 30 percent (Ref. 11). No data were available from which to infer the shape of the distribution.

The distribution of fluence was assumed to be a normal distribution. The mean is the attenuated fluence at the inner wall, and the standard deviation is taken to be a fraction of the mean. The fluence at the inner wall and the fraction of the mean are input parameters.

3.5 FRACTURE TOUGHNESS (K_{Ic} AND K_{Ia})

The mean value functions of the fracture toughness for crack initiation (K_{Ic}) and arrest (K_{Ia}) as a function of $T - RT_{NDT}$ were obtained by nonlinear regression (Ref. 4). The mean curves that were obtained are

$$K_{Ic} = \begin{cases} 36.2 + 49.4e^{.0104(T - RT_{NDT})} & , \quad T - RT_{NOT} \leq -50 \\ 55.1 + 28e^{.2014(T - RT_{NDT})} & , \quad T - RT_{NDT} > 50 \end{cases}$$

and

$$K_{Ia} = \begin{cases} 19.9 + 43.9e^{.00993(T - RT_{NDT})} & , \quad T - RT_{NDT} \leq 50 \\ 70.1 + 6.50e^{.0196(T - RT_{NDT})} & , \quad T - RT_{NDT} > 50 \end{cases}$$

The mean curves are truncated at some maximum stress intensity value defined by the user [200 ksi $\sqrt{\text{in.}}$ was used in the NRC staff evaluation of PTS (Ref. 4)]. The distributions of K_{Ic} and K_{Ia} about their mean values were assumed to be normal, with a standard deviation of 10 percent of the mean value. Use of the 10-percent deviation is suggested in Ref. 12.

4.0 VISA COMPUTER CODE

The VISA code is expected to be used in a number of different applications. Because the results of a simulation analysis depend critically on the relationships between the stochastic variables and the way in which stochasticity enters the calculation, a detailed description of the logic of the code is presented in this chapter. To facilitate program modifications by the user, VISA is described using the variable names used in the code.

The logic of the main program is outlined in Section 4.1. Capsule descriptions of each of the subroutines are given in Section 4.2. The code names of the important physical variables are defined with the descriptions. A flow chart of VISA is provided in Figure 4.1.

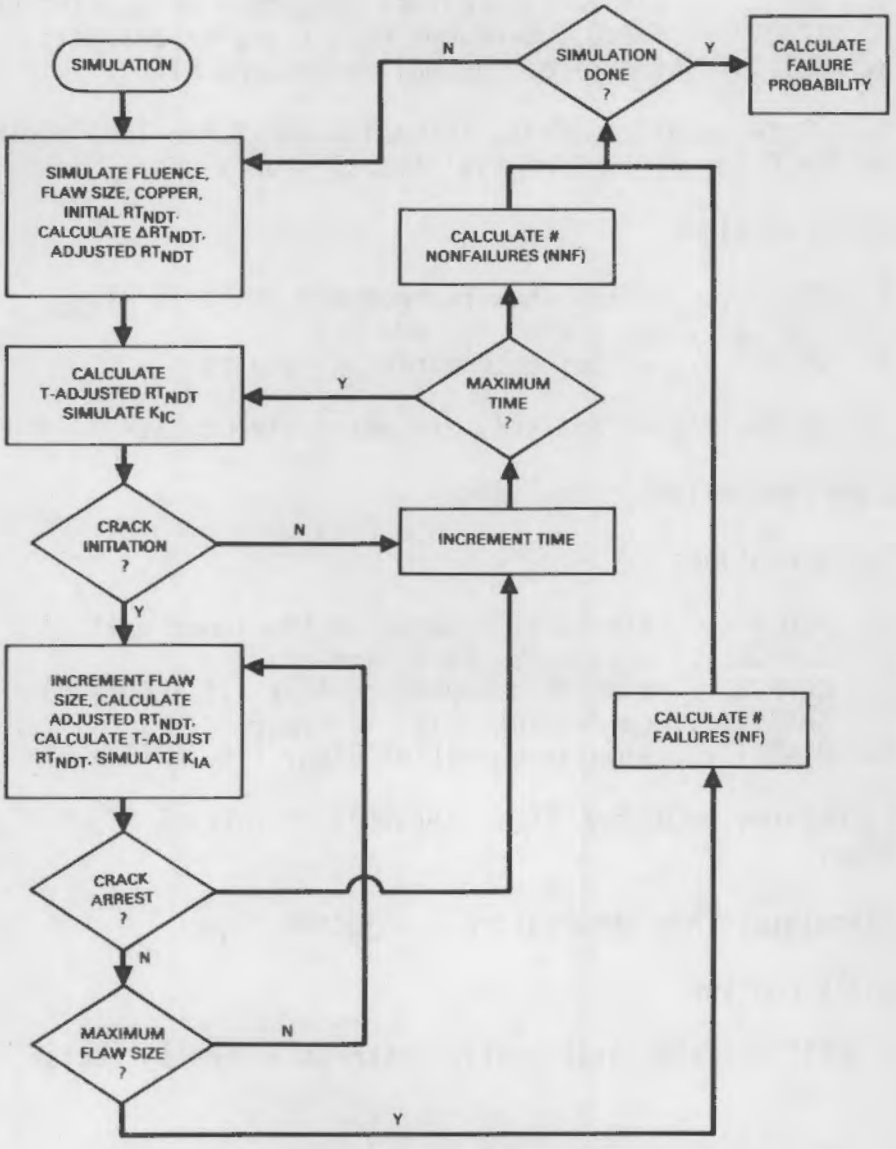

FIGURE 4.1. Flow Chart for Simulation Model

4.1 MAIN ROUTINE OUTLINE

As the outline below of the main program indicates, VISA does the following routines:

1. Establishes all common blocks

2. Opens output file VOUT.DAT

3. Calls routines to input and output analysis specifications from file VISA.DAT

4. Performs deterministic analysis

   A. Calls routines

      1. SPKI.... calculates pressure component of applied stress
      2. TPOLY or TEXP.... performs heat transfer analysis
      3. SKIT.... calculates thermal stress and KIT

   B. Calculates applied stress intensity (APKI for longitudinal flaws or APKIC for circumferential flaws) = pressure + thermal stress

   C. Calls routines

      1. ARRAY.... establishes fluence and shift in RT_{NDT}
      2. SMAT..... calculates K_{IC} and K_{IA}
      3. WRITE1.... writes deterministic results

5. Ends if probabilistic analysis are not desired; KSIM = 1

6. Performs probabilistic analysis

   A. Calls routines

      1. FLUENC.... simulates fluence at the inner wall
      2. SCRACK.... simulates crack size
      3. COPPER.... simulates copper content (if IFCU = 0)
      4. SHIFT..... calculates shift in RT_{NDT}
      5. RTNDTI.... simulates initial RT_{NDT} (if IFRTI = 0)

   B. Calculates adjusted RT_{NDT} (ARTNDT) = initial RT_{NDT} + shift in RT_{NDT}

   C. Calculates TA = temperature - adjusted RT_{NDT}

   D. Calls routine

      SCSIF.... simulates critical stress intensity factor

E. Checks for crack initiation. Crack initiates if:

applied stress > critical stress intensity factor
(APKI > K_{Ic})

F. If no crack initiates, VISA:

1. Adds one to TIMES
2. If TIMES ≤ 10 transfers to 6C (next time step)
3. If done with simulations, transfers to 6H
4. Sets TIMES = 1
5. Transfers to 6A (next simulation run)

G. It crack initiates, VISA:

1. Calls routine

WRITE2.... writes crack initiation data

2. Increments crack depth
3. Checks for crack arrest

a. Calls routine

SHIFT.... calculates shift in RT_{NDT}

b. Calculates adjusted RT_{NDT} = initial RT_{NDT} + shift in RT_{NDT}
c. Calculates TA = temperature - adjusted RT_{NDT}
d. Calls routine

SKIA.... calculates K_{IA}

1. If crack arrest occurs, VISA:

a. Checks for plastic instability of remaining ligament
b. Writes out crack arrest data
c. Adds one to TIMES
d. If TIMES ≤ 10 transfers to 6C (next time step)
e. If done with simulations, transfers to 6H
f. Writes final arrest data
g. Sets TIMES = 1
h. Transfers to 6 (next simulation run)

2. If no crack arrest occurs, VISA compares crack depth to maximum crack depth

a. If crack depth equals maximum crack depth, VISA:

1. Writes failure data
2. If done with simulations, transfers to 6H
3. Sets TIMES = 1
4. Transfers to 6 (next simulation run)

b. If crack depth is less than maximum crack depth, VISA:

1. Transfers to 6G2 (next crack depth)

H. Writes final simulation data.

4.2 SUBROUTINE DESCRIPTIONS

As the outline below indicates, the subroutine READ does the following:

1. Opens input file VISA.DAT
2. Inputs all variables (see Section 5.1)
3. Defines variables

a. AL..... The four roots of $\alpha \tan(\alpha) = C$

b. ZZ..... The five influence functions for longitudinal flaws

c. ZZC..... The five influence functions for circumferential flaws

d. Z..... The 32 crack depths (1/8, 1/4, 2/4, ..., 31/4)

e. ZQ..... Quarter points at wall thickness

f. ISEED.... Upper 16 bits of multiplier for random number generator

g. I2..... Lower 16 bits of multiplier for random number generator

h. PI..... 3.1416.

The subroutine ECHO:

1. Writes out input data.

4.2.1 Deterministic Analysis Subroutine

Outlines of the deterministic analysis subroutines are given below.

SPKI:

1. Calculates pressure (PRES)

2. Calculates pressure component of applied stress (PKI for longitudinal flaws and PKIC for circumferential flaws)

TPOLY: For polynomial representation of water temperature

1. Calculates water temperature at each time step (TWATER)

2. Performs heat transfer and calculates quarter-point temperatures in RPV wall (TQ)

TEXP: For exponential representation of water temperature

1. Calculates water temperature at each time step (TWATER)

2. Performs heat transfer analysis and calculates quarter-point temperatures in RPV wall (QC)

SKIT:

1. Calculates temperature at crack tips (T)

2. Calculates stress at crack tips (STRESS)

3. Calculates thermal stress intensity (TK for longitudinal flaws and TKC for circumferential flaws)

ARRAY:

1. Calculates fluence at crack tips (FLA)

2. Calculates square root of fluence (SQRFLA)

3. Calculates maximum shift in RT_{NDT} at crack tips (CRTS)

4. Establishes arrays to calculate drop in CV (charpy V-notch) upper-shelf energy (DSEPF, DSEPMF)[a]

5. Calculates shift in RT_{NDT} for constant copper value (SRT)

SMAT:

1. Calculates K_{Ic} (CKIC) and K_{Ia} (CKIR)

WRITE1:

1. Writes out results of deterministic analysis.

4.2.2 Probabilistic Analysis Subroutine

Outlines of the probabilistic analysis subroutines are given below.

[a]Not used in current version of the code.

FLUENCE:

1. Simulates ID fluence (SFID)

SCRACK:

1. Simulates crack size
2. Defines variables

   a. A..... crack depth
   b. C..... index for crack size

COPPER:

1. Simulates copper content (CU)

SHIFT:

1. Calculates fluence at crack depth based on simulated fluence at ID (FLA)
2. Calculates shift in RT_{NDT} (RTS)

RTNDTI:

1. Simulates initial RT_{NDT} (RTI)

SCSIF:

1. Simulates critical stress intensity value (allowable stress ALKI)
2. Sets ISHELF

   equal to 1 if critical stress intensity factor value is on upper shelf

   equal to 0 if critical stress intensity factor value is not on upper shelf

WRITE2:

1. Writes out results of simulation analysis

SKIA:

1. Simulates KIA (CKIA)

NORMAL: (XMEAN, SIGMA, Y)

1. Calls random number generator RANF(I1,I2,R)
2. Returns normalized random number.

5.0 USER'S GUIDE

5.1 INPUT DESCRIPTION

The deterministic input to VISA consists of constants describing the physical characteristics of the vessel, pressure, and temperature during the transient; flags that identify what kind of analysis is to be performed; and certain constants for these analyses.

The probabilistic input includes a flag to indicate if the probabilistic analysis is desired. If probabilistic analysis is desired, then this input also includes the means and standard deviations of copper and initial RT_{NDT}, and a flag to indicate whether simulations are to be performed on copper and initial RT_{NDT}.

Input to VISA is from a file named VISA.DAT. The format of this file is detailed in this section. It is assumed that the file has been created using a software editor or is a card image file. If the code is to be used in a card-oriented, batch-processing environment, the READ statements can be modified to read directly from a card reader.

INPUT FILE DESCRIPTION

Record	Columns	Format	Program Variable	Description
1	1-10	F10.3	TH	Vessel wall thickness, inches
	11-20	F10.3	YLDIRR	Irradiated yield stress, ksi (not used in present version of VISA)
	21-30	F10.3	SIGF	Material flow stress, ksi
	31-40	1E10.3	FID	Fluence at vessel ID, neut/cm^2 (E > 1 MEV)
2	1-10	F10.3	CU	Copper content for use in deterministic analysis, percent
	11-20	F10.3	RTI	Initial RT_{NDT} for use in deterministic analysis, ^oF
3	1-10	F10.3	PDATA(1)	Pressure at time = 0, ksi
	11-20	F10.3	PDATA(2)	Pressure 1/4 of the time through transient, ksi
	21-30	F10.3	PDATA(3)	Pressure 1/2 of the time through transient, ksi
	31-40	F10.3	PDATA(4)	Pressure 3/4 of the time through transient, ksi
	41-50	F10.3	PDATA(5)	Pressure at the end of the transient, ksi
4	1-10	I10	MODEL	Check for model for water temperature 1 → exponential 0 → polynomial
	11-20	I10	CONSTK	Check for thermal diffusivity 1 → constant 0 → function of temperature
	21-30	I10	CONSTE	Check for $E\alpha/(1-\nu)$ 1 → constant 0 → function of temperature

Record	Columns	Format	Program Variable	Description
	31-40	I10	LORC	Check for flaw orientation 1 → circumferential 0 → longitudinal
	41-50	I10	IFWPS	Check for warm prestress 1 → warm prestress 0 → no warm prestress
5	(Delete this record for function $E\alpha/(1-\nu)$ option)			
	1-10	F10.3	EDATA	Constant value of $E\alpha/(1-\nu)$, ksi
6	1-10	F10.3	TO	Initial water temperature, ^{o}F
	11-20	F10.3	DT	Change in water temperature, ^{o}F (must be negative for temperature drop)
	21-30	F10.3	BE	Decay constant, min^{-1}
6	(For polynomial modeling in water temperature)			
	1-10	F10.3	TINT	Initial water temperature, ^{o}F
	11-20	F10.3	TDATA(1)	Temperature at time = 0, ^{o}F
	21-30	F10.3	TDATA(2)	Temperature 1/4 of the time through transient, ^{o}F
	31-40	F10.3	TDATA(3)	Temperature 1/2 of the time through transient, ^{o}F
	41-50	F10.3	TDATA(4)	Temperature 3/4 of the time through transient, ^{o}F
	51-60	F10.3	TDATA(5)	Temperature at the end of transient, ^{o}F
7	1-10	F10.3	TMAX	Length of transient analyzed, minutes

Record	Columns	Format	Program Variable	Description
	11-20	F10.3	ROOT[a]	Specifies values for the dimensions parameter C of transcendental equation $\alpha \tan(\alpha) = C$
	21-30	F10.3	KO	Thermal diffusivity, $in.^2/min$
8	1-10	I10	KSIM	Check for probabilistic option 1 → do not perform 0 → perform

(Delete Records 9 and 10 if probabilistic analysis is not to be performed)

[a] The dimensionless parameter ROOT has the following definition:

$$C = \frac{(\text{Effective Heat Transfer Coefficient}) \cdot (\text{Wall Thickness})}{\text{Thermal Conductivity}}$$

where a consistent set of units is

Effective Heat Transfer Coefficient, $BTU/hr\text{-}ft^2\text{-}^oF$
Wall Thickness, ft
Thermal Conductivity, $BTU/hr\text{-}ft\text{-}^oF$.

The user must select from five discrete values of C through input of values for ROOT of 0.0, 10.0, 20.0, 40.0 or 60.0. The specified values of ROOT result in the following values assigned to the parameter C:

Specified Value of ROOT	Resulting Value of C
0.0 (zero)	6.0 (six)
10.0	10.0
20.0	20.0
40.0	40.0
60.0	60.0

Attempts to specify other values of ROOT will result in an incorrect solution or abnormal termination of the computer run.

INPUT FILE DESCRIPTION (Cont'd)

Record	Columns	Format	Program Variable	Description
9	1-10	F10.3	XMNCU	Mean copper content, weight percent
	11-20	F10.3	SIGCU	Standard deviation of copper content, weight percent
	21-30	F10.3	XMNRTI	Mean initial RT_{NDT}, ^{o}F
	31-40	F10.3	SIGRTI	Standard deviation of initial RT_{NDT}, ^{o}F
	41-50	F10.3	SIGFID	Standard deviation of fluence, neutrons/cm^2
	51-60	F10.3	USKIC	Upper-shelf maximum stress intensity, ksi $\sqrt{in.}$
	61-70	I10	NS	Number of simulations desired
10	1-10	I10	IFCU	Check for copper content 1 → constant value previously entered 0 → simulate
	11-20	I10	IFRTI	Check for initial RT_{NDT} 1 → constant value previously entered 0 → simulate

5.2 SAMPLE OUTPUT

An edited list of the output from a simulation analysis is given in this section. The test case is the same one used in Appendix B to compare VISA to OCA-I. The actual output would include listings of the stress intensity factors for each time point in the transient, and descriptions for each crack that initiated propagation. For brevity, only the first and last time points and only a few sample flaw descriptions are included in the list.

****** REACTOR PRESSURE VESSEL PRESSURIZED THERMAL SHOCK ANALYSIS ******

*** INPUT DATA ***

SIMULATION ANALYSIS HAS BEEN PERFORMED

EXPONENTIAL MODELING OF WATER TEMPERATURE HAS BEEN USED

A CONSTANT THERMAL DIFFUSIVITY OF 9.820E-01 IN**2/M IN HAS BEEN USED

A CONSTANT VALUE OF 3.100E-01 HAS BEEN USED FOR (E*ALPHA/1-MU)

VESSEL RAD	= 8.5000E+01	IN
WALL THICKNESS	= 8.5000E+00	IN
COPPER CONTENT	= 3.4000E-01	
INITIAL RTNDT	= 3.0000E+01	
UPPER SHELF KIC	= 2.0000E+02	
ID FLUENCE	= 2.0000E+19	NUET/CM**2

TIME PERIOD ANALYZED = 9.6000E+01 MIN

INITIAL WATER TEMP	= 5.5000E+02	(F)
DELTA T	= 3.0000E+02	(F)
DECAY CONSTANT	= 1.5000E-01	

FIRST FOUR ROOTS OF ALPHA*TAN(ALPHA) = C WHEN C = 0. ARE:

1.3496	4.1116	6.9924	9.9667

THE INFLUENCE FUNCTIONS USED ARE: Z(X,Y) =

1.1220	0.9513	-0.6240	8.3306
0.6825	0.3704	-0.0832	2.8251
0.5255	0.2011	0.0313	1.4250
0.4414	0.1337	0.0386	0.8806
0.3863	0.0989	0.0437	0.5951
1.1220	-0.0100	3.0000	0.0000
0.6825	-0.0565	1.2229	0.0000
0.5255	-0.1045	0.7471	0.0000
0.4414	-0.1196	0.5535	0.0000
0.3863	-0.0521	0.3991	0.0000

IRR YIELD STRESS(KSI) = 8.000E+01
INITIAL UPPER SHELF CV ENERGY (FT-LBS) = 0.00000E-01
FLOW STRESS(KSI) = 9.000E+01
A CONSTANT IRTNDT VALUE OF 3.00000E+01 HAS BEEN USED

STATISTICAL PARAMETERS

COPPER DISTRIBUTION	IRTNDT DISTRIBUTION	FLUENCE DISTRIBUTION
MEAN = 1.00D00E-01	MEAN = 3.00000E+01	MEAN = 2.00000E+19
SIG = 2.50000E-02	SIG = 1.50000E+01	SIG = 6.00000E+18

NUMBER OF SIMULATIONS REQUESTED = 500000

THERMAL SHOCK ANALYSIS FOR EXPONENTIAL DECAY OF WATER TEMPERATURE

LONGITUDINALLY ORIENTED FLAWS

T= 9.60 MIN
PRES= 2.00 KSI WATER TEMP = 321.08 DEG F

DEPTH (IN)	TEMP (F)	T STR	KIT	KIP (KSI*IN**.5)	LB KIC	KIA	APP K
0.125	400.0	36.8	26.8	15.0	89.1	52.3	41.8
0.250	406.5	34.6	37.0	21.4	100.1	55.9	58.4
0.500	418.7	30.3	49.8	30.9	127.7	64.2	80.7
0.750	430.1	26.3	58.0	38.8	164.3	74.2	96.8
1.000	440.6	22.6	63.9	45.9	200.0	86.1	109.7
1.250	450.4	19.2	68.2	52.7	200.0	100.1	120.9
1.500	459.5	16.1	71.6	59.5	200.0	116.3	131.1
1.750	467.9	13.1	74.5	66.5	200.0	135.0	141.0
2.000	475.7	10.4	77.1	73.8	200.0	156.3	150.9
2.250	482.9	7.9	79.7	81.8	200.0	180.2	161.5
2.500	489.5	5.6	82.4	90.4	200.0	200.0	172.9
2.750	495.6	3.5	85.5	100.0	200.0	200.0	185.4
3.000	501.1	1.5	88.9	110.6	200.0	200.0	199.5
3.250	506.2	-0.2	92.8	122.5	200.0	200.0	215.3
3.500	510.9	-1.9	97.3	135.8	200.0	200.0	233.1
3.750	515.2	-3.4	102.4	150.7	200.0	200.0	253.1
4.000	519.1	-4.7	108.2	167.4	200.0	200.0	275.6
4.250	522.6	-6.0	114.5	186.2	200.0	200.0	300.7
4.500	525.8	-7.1	121.6	207.1	200.0	200.0	328.7
4.750	528.7	-8.1	129.3	230.4	200.0	200.0	359.7
5.000	531.3	-9.0	137.5	256.4	200.0	200.0	393.9
5.250	533.6	-9.8	146.4	285.1	200.0	200.0	431.5
5.500	535.7	-10.5	155.7	317.0	200.0	200.0	472.7
5.750	537.5	-11.2	165.5	352.1	200.0	200.0	517.5
6.000	539.1	-11.7	175.6	390.7	200.0	200.0	566.2
6.250	540.6	-12.2	186.0	433.0	200.0	200.0	619.0
6.500	541.8	-12.6	196.6	479.3	200.0	200.0	675.9
6.750	542.8	-13.0	207.2	529.8	200.0	200.0	737.0
7.000	543.6	-13.3	217.9	584.7	200.0	200.0	802.6
7.250	544.3	-13.5	228.3	644.4	200.0	200.0	872.7
7.500	544.8	-13.7	238.6	709.0	200.0	200.0	947.6
7.750	545.2	-13.8	248.4	778.8	200.0	200.0	1027.3

T=96.00 MIN

PRES= 2.00 KSI WATER TEMP = 250.00 DEG F

DEPTH (IN)	TEMP (F)	T STR	KIT	KIP (KSI*IN**.5)	LB KIC	KIA	APP K
0.125	259.9	6.8	4.9	15.0	36.6	30.1	19.9
0.250	260.7	6.5	6.9	21.4	36.8	30.3	28.3
0.500	262.3	6.0	9.5	30.9	37.3	30.7	40.4
0.750	263.9	5.5	11.3	38.8	37.9	31.0	50.1
1.000	265.4	5.0	12.8	45.9	38.6	31.5	58.6
1.250	267.0	4.4	14.0	52.7	39.3	31.9	66.6
1.500	268.5	3.9	15.0	59.5	40.1	32.4	74.5
1.750	269.9	3.4	15.9	66.5	41.0	32.9	82.4
2.000	271.4	3.0	16.8	73.8	42.0	33.5	90.6
2.250	272.8	2.5	17.6	81.8	43.1	34.1	99.4
2.500	274.1	2.0	18.5	90.4	44.3	34.7	109.0
2.750	275.5	1.6	19.5	100.0	45.7	35.4	119.5
3.000	276.7	1.1	20.5	110.6	47.2	36.1	131.1
3.250	278.0	0.7	21.6	122.5	48.8	36.9	144.1
3.500	279.2	0.3	22.8	135.8	50.6	37.7	158.6
3.750	280.3	-0.1	24.2	150.7	52.0	38.4	174.9
4.000	281.5	-0.5	25.7	167.4	56.9	40.5	193.1
4.250	282.5	-0.8	27.3	186.2	62.6	42.8	213.5
4.500	283.5	-1.2	29.1	207.1	69.5	45.5	236.1
4.750	284.5	-1.5	31.0	230.4	77.6	48.4	261.4
5.000	285.4	-1.8	33.0	256.4	87.1	51.7	289.4
5.250	286.2	-2.1	35.2	285.1	98.0	55.2	320.3
5.500	287.0	-2.3	37.4	317.0	110.5	59.1	354.4
5.750	287.7	-2.6	39.8	352.1	124.8	63.3	391.8
6.000	288.4	-2.8	42.2	390.7	140.9	67.9	432.9
6.250	289.0	-3.0	44.7	433.0	158.8	72.7	477.7
6.500	289.6	-3.2	47.2	479.3	178.8	77.9	526.5
6.750	290.0	-3.4	49.7	529.8	200.0	83.4	579.5
7.000	290.5	-3.5	52.3	584.7	200.0	89.2	637.0
7.250	290.8	-3.6	54.7	644.4	200.0	95.3	699.1
7.500	291.1	-3.7	57.1	709.0	200.0	101.6	766.1
7.750	291.3	-3.8	59.4	778.8	200.0	108.1	838.2

CIRCUMFERENTIALLY ORIENTED FLAWS

T= 9.60 MIN
PRES= 2.00 KSI WATER TEMP = 321.08 DEG F

DEPTH (IN)	TEMP (F)	T STR	KIT	KIP	LB KIC	KIA	APP K
				(KSI*IN**.5)			
0.125	400.0	36.8	26.5	7.0	89.1	52.3	33.6
0.250	406.5	34.6	36.2	10.0	100.1	55.9	46.2
0.500	418.7	30.3	47.8	14.2	127.7	64.2	62.0
0.750	430.1	26.3	54.9	17.6	164.3	74.2	72.5
1.000	440.6	22.6	59.7	20.6	200.0	86.1	80.3
1.250	450.4	19.2	63.0	23.5	200.0	100.1	86.5
1.500	459.5	16.1	65.5	26.3	200.0	116.3	91.9
1.750	467.9	13.1	67.4	29.2	200.0	135.0	96.7
2.000	475.7	10.4	68.9	32.2	200.0	156.3	101.2
2.250	482.9	7.9	70.2	35.3	200.0	180.2	105.5
2.500	489.5	5.6	71.2	38.6	200.0	200.0	109.8
2.750	495.6	3.5	72.1	42.1	200.0	200.0	114.2
3.000	501.1	1.5	72.9	45.8	200.0	200.0	118.7
3.250	506.2	-0.2	73.7	49.7	200.0	200.0	123.4
3.500	510.9	-1.9	74.3	53.9	200.0	200.0	128.3
3.750	515.2	-3.4	74.9	58.4	200.0	200.0	133.3
4.000	519.1	-4.7	75.4	63.2	200.0	200.0	138.6
4.250	522.6	-6.0	75.8	68.2	200.0	200.0	144.0
4.500	525.8	-7.1	76.1	73.6	200.0	200.0	149.7
4.750	528.7	-8.1	76.2	79.3	200.0	200.0	155.5
5.000	531.3	-9.0	76.2	85.4	200.0	200.0	161.6
5.250	533.6	-9.8	76.0	91.8	200.0	200.0	167.8
5.500	535.7	-10.5	75.6	98.6	200.0	200.0	174.2
5.750	537.5	-11.2	75.0	105.7	200.0	200.0	180.7
6.000	539.1	-11.7	74.1	113.3	200.0	200.0	187.4
6.250	540.6	-12.2	73.0	121.3	200.0	200.0	194.2
6.500	541.8	-12.6	71.6	129.6	200.0	200.0	201.2
6.750	542.8	-13.0	69.8	138.4	200.0	200.0	208.2
7.000	543.6	-13.3	67.8	147.6	200.0	200.0	215.4
7.250	544.3	-13.5	65.4	157.3	200.0	200.0	222.7
7.500	544.8	-13.7	62.6	167.4	200.0	200.0	230.0
7.750	545.2	-13.8	59.5	178.0	200.0	200.0	237.5

T=96.00 MIN

PRES= 2.00 KSI WATER TEMP = 250.00 DEG F

DEPTH (IN)	TEMP (F)	T STR	KIT	KIP (KSI*IN**.5)	LB KIC	KIA	APP K
0.125	259.9	6.8	4.9	7.0	36.6	30.1	11.9
0.250	260.7	6.5	6.7	10.0	36.8	30.3	16.7
0.500	262.3	6.0	9.1	14.2	37.3	30.7	23.3
0.750	263.9	5.5	10.7	17.6	37.9	31.0	28.3
1.000	265.4	5.0	12.0	20.6	38.6	31.5	32.6
1.250	267.0	4.4	12.9	23.5	39.3	31.9	36.4
1.500	268.5	3.9	13.8	26.3	40.1	32.4	40.1
1.750	269.9	3.4	14.5	29.2	41.0	32.9	43.7
2.000	271.4	3.0	15.1	32.2	42.0	33.5	47.3
2.250	272.8	2.5	15.6	35.3	43.1	34.1	51.0
2.500	274.1	2.0	16.2	38.6	44.3	34.7	54.8
2.750	275.5	1.6	16.6	42.1	45.7	35.4	58.7
3.000	276.7	1.1	17.1	45.8	47.2	36.1	62.9
3.250	278.0	0.7	17.5	49.7	48.8	36.9	67.2
3.500	279.2	0.3	17.9	53.9	50.6	37.7	71.8
3.750	280.3	-0.1	18.2	58.4	52.0	38.4	76.6
4.000	281.5	-0.5	18.5	63.2	56.9	40.5	81.7
4.250	282.5	-0.8	18.8	68.2	62.6	42.8	87.0
4.500	283.5	-1.2	19.1	73.6	69.5	45.5	92.7
4.750	284.5	-1.5	19.2	79.3	77.6	48.4	98.6
5.000	285.4	-1.8	19.4	85.4	87.1	51.7	104.7
5.250	286.2	-2.1	19.4	91.8	98.0	55.2	111.2
5.500	287.0	-2.3	19.4	98.6	110.5	59.1	118.0
5.750	287.7	-2.6	19.4	105.7	124.8	63.3	125.1
6.000	288.4	-2.8	19.2	113.3	140.9	67.9	132.5
6.250	289.0	-3.0	19.0	121.3	158.8	72.7	140.3
6.500	289.6	-3.2	18.7	129.6	178.8	77.9	148.3
6.750	290.0	-3.4	18.3	138.4	200.0	83.4	156.7
7.000	290.5	-3.5	17.8	147.6	200.0	89.2	165.4
7.250	290.8	-3.6	17.2	157.3	200.0	95.3	174.5
7.500	291.1	-3.7	16.5	167.4	200.0	101.6	183.9
7.750	291.3	-3.8	15.7	178.0	200.0	108.1	193.7

THIS IS SIMULATION NUMBER 322591

CRACK INITIATION OCCURRED 19.20 MIN INTO TRANSIENT

THE FLAW IS LONGITUDINALLY ORIENTED

PRESSURE (KSI) = 2.0000E+00
TEMPERATURE (F) = 4.2248E+02
CRACK LENGTH (IN) = 2.5000E+00
PERCENT COPPER = 1.0534E-01
FLUENCE AT CRACK TIP (N/CM**2) = 1.0810E+19
FLUENCE AT VESSEL ID (N/CM**2) = 2.0000E+19
INITIAL RTNDT (F) = 1.5665E+00
SHIFT IN RTNDT (F) = 0.0000E-01
APPLIED STRESS INTENSITY VALUE (KSI*SQRT(IN)) = 1.9629E+02
CRITICAL STRESS INTENSITY VALUE (KSI*SQRT(IN)) = 1.7411E+02
PRESSURE COMPONENT OF APKI (KSI*SQRT(IN)) = 9.0428E+01
RESIDUAL COMPONENT OF APKI (KSI*SQRT(IN)) = 0.0000E-01
THERMAL COMPONENT OF APKI (KSI*SQRT(IN)) = 1.0586E+02

SIMULATED ID FLUENCE = 2.4667E+19

THE CRITICAL STRESS INTENSITY VALUE IS ON THE UPPER SHELF

PERCENTAGE DROP IN UPPER SHELF CV ENERGY = 0.0000E-01
IRR UPPER SHELF KIC MEAN VLAUE (KSI*SQRT(IN)) = 2.0000E+02

THE CRACK ARRESTED AT A DEPTH OF 3.0000E+00 INCHES

THE ARREST TOUGHNESS = 2.4047E+02 KSI*SQRT(IN)

THE CRACK DID NOT PENETRATE THROUGH WALL
THIS IS SIMULATED CRACK INITIATION NUMBER 1

500000 SIMULATIONS HAVE BEEN MADE

THE FAILURE RATE FOR 500000 SIMULATIONS IS 0.00000E-01

THE PROBABILITY OF CRACK INITIATION IS 2.000000E-06

A 95% CONFIDENCE INTERVAL FOR THE CALCULATED FAILURE RATE IS
0.00000E-01

6.0 REFERENCES

1. Advisory Committee on Reactor Safeguards. 1974. Report on the Integrity of Reactor Vessels for Light-Water Power Reactors. WASH-1285, U.S. Atomic Energy Commission, Washington, D.C.*

2. U.S. Atomic Energy Commission Regulatory Staff. 1974. Technical Report on Analysis of Pressure Vessel Statistics From Fossil-Fueled Power Plant Service and Assessment of Reactor Vessel Reliability in Nuclear Power Plant Service. WASH-1318, U.S. Atomic Energy Commission, Washington, D.C.*

3. American Society of Mechanical Engineers (ASME). Boiler and Pressure Vessel Code, The American Society of Mechanical Engineers, Philadelphia, Pennsylvania.

4. Policy Issue from J. W. Dircks to NRC Commissioners. "Enclosure A: NRC Staff Evaluation of Pressurized Thermal Shock, November 1982." SECY-82-465, November 23, 1982. Division of Nuclear Reactor Regulation, U.S. Nuclear Regulatory Commission, Washington, D.C.

5. Labbens, R., A. Pellissier-Tanon and J. Heliot. 1976. "Practical Method for Calculating Stress-Intensity Factors Through Weight Functions." In Mechanics of Crack Growth, pp. 368-384. ASTM STP-590, American Society for Testing and Materials.

6. Heliot, J., R. C. Labbens and A. Pellissier-Tanon. 1978. "Semi-Elliptical Cracks in the Mendional Plane of a Cylinder Subjected to Stress Gradients, Calculation of Stress Intensity Factors by the Boundary Integral Equations Method," XIth National Symposium on Fracture Mechanics, Blacksburg, Virginia.

7. Iskander, S. K., R. D. Cheverton, D. G. Ball. 1981. A Code for Calculating the Behavior of Flaws on the Inner Surface of a Pressure Vessel Subjected to Temperature and Pressure Transients. NUREG/CR-2113, ORNL-NUREG-84, OCA-I, U.S. Nuclear Regulatory Commission, Washington, D.C.*

8. U.S. Nuclear Regulatory Commission. 1977. "Effects of Residual Elements in Predicting Radiation Damage to Reactor Vessel Materials." In Regulatory Guide 1.99, Revision 1, U.S. Nuclear Regulatory Commission, Washington, D.C.*

*Available for purchase from the NRC/GPO Sales Program, U.S. Nuclear Regulatory Commission, Washington, D.C. 10555; and/or the National Technical Information Service, Springfield, Virginia 22161.

9. Vesely, W. E., E. K. Lynn and F. F. Goldberg. 1978. The Octavia Computer Code: PWR Reactor Pressure Vessel Failure Probabilities Due to Operationally Caused Pressure Transients." NUREG-0258, U.S. Nuclear Regulatory Commission, Washington, D.C.*

10. Combustion Engineering, Inc. 1981. Evaluation of Pressurized Thermal Shock Effects Due to Small Break LOCA's with Loss of Feedwater for the Combusion Engineering NSSS. CEN-189, Windsor, Connecticutt.

11. McElroy, W. N., A. I. Davis and R. Gold. 1981. Surveillance Dosimetry of Operating Power Plants. HEDL-SA-2546, Hanford Engineering Development Laboratory, Richland, Washington.

12. Marshall, W. 1976. An Assessment of the Integrity of PWR Pressure Vessels. Study Group Report, Services Branch, United Kingdom Atomic Energy Agency, London.

APPENDIX A

EQUATIONS FOR DETERMINISTIC ANALYSES

APPENDIX A

EQUATIONS FOR DETERMINISTIC ANALYSES

This appendix describes the development of equations that are used in the deterministic fracture mechanics portion of the VISA computer code. The derivations of these equations were made by R. W. Klecker, NRC, in 1978 and were recently adapted for use in the VISA code. Since the basic approach and assumptions are emphasized in the body of this report, the focus of this appendix will be to document the derivations and the details of the resulting equations. The greatest attention will be on the transient temperature analysis. The stress analyses and stress intensity calculations will be reviewed only briefly, since they follow either well-known approaches or use results that are well documented in the literature.

The final topic of the appendix is the specific temperature-dependent representation of material properties, which the user of VISA may choose to utilize by suitable selection of control parameters of the input data.

NOMENCLATURE

h = heat transfer coefficient

k = thermal conductivity

κ = thermal diffusivity

E = modulus of elasticity

α = linear coefficient of expansion

ν = Poisson's ratio

ℓ = wall thickness

x = distance from heated or cooled surface

a = crack depth

t = time

$\left.\begin{aligned} \xi &= \frac{x}{\ell} \\ \alpha &= \frac{a}{\ell} \\ \tau &= \frac{\kappa t}{\ell^2} \end{aligned}\right\}$ dimensionless parameters

T_0 = initial water and metal temperature

$T_W(t)$ = water temperature versus time

$T(x,t)$ = metal temperature versus time and distance

$\phi(t) = T_W(t) - T_0$

$v(x,t) = T(x,t) - T_0$

$F(x,t)$ = special case of $v(x,t)$

TRANSIENT TEMPERATURE DISTRIBUTIONS

In equations for the temperature distributions, the wall of the vessel is approximated by a flat-slab geometry. The wall of the slab is of a single material, and thus does not treat the effect of surface cladding. Also, the heat transfer coefficient, h, is taken to be constant and does not vary with time in the one-dimensional analysis. At the start of the temperature transient, the slab is taken to be at a uniform temperature. A series solution is developed for temperatures in the vessel wall as a function of time. Parameters for up to six series terms are given in this appendix, although only four terms are actually used in the VISA computer program.

Governing Equations for Temperature Distribution

For a particular transient, the water temperature is assumed to vary as

$$T_W(t) = T_0 + \phi(t) \tag{1}$$

where

$T_W(t)$ = water temperature versus time

T_0 = initial water and metal temperature

$\phi(t)$ = variation in water temperature from T_0

t = time

During the transient, the temperature of the vessel wall is defined as

$$T(x,t) = T_0 + v(x,t) \quad , \quad v(x,0) = 0 \tag{2}$$

where

$T(x,t)$ = transient wall temperature

$v(x,t)$ = transient wall temperature variation from T_0

x = distance into the wall measured from the heated or cooled surface

For calculational convenience, the following dimensionless parameters are used:

$$\xi = \frac{x}{\ell} = \text{dimensionless distance} \tag{3}$$

$$\tau = \frac{\kappa t}{\ell^2} = \text{dimensionless time} \tag{4}$$

where

ℓ = wall thickness (including clad)

κ = thermal diffusivity of the metal .

Equations (1) and (2) then become, respectively,

$$T_W(\tau) = T_0 + \phi(\tau) \tag{5}$$

$$T(\xi,\tau) = T_0 + v(\xi,\tau) \quad , \quad v(\xi, 0) = 0 \ . \tag{6}$$

The basic equation for heat conduction in a slab requires that $v(\xi,\tau)$ must satisfy

$$\frac{\partial v}{\partial \tau} = \frac{\partial^2 v}{\partial \xi^2} \tag{7}$$

In addition, for a metal slab heated or cooled on the surface $\xi = 0$ and insulated at $\xi = 1$, the boundary conditions require no heat flow at the insulated surface,

$$\frac{\partial v}{\partial \xi}\ (1,\tau) = 0 \tag{8}$$

and the following heat flow balance must exist at the heated or cooled surface

$$\frac{\partial v}{\partial \xi}\ (0,\tau) = C[v(0,\tau) - \phi(\tau)] \tag{9}$$

where

$$C = \frac{h\ell}{k} \ , \text{ a dimensionless constant} \tag{10}$$

h = heat transfer coefficient

k = thermal conductivity of the metal .

The initial condition of Equation (6) requires

$$v(\xi,0) = 0 \quad . \tag{11}$$

The metal temperature distribution for the assumed geometry versus time following a step change in water temperature is derived in many texts on heat transfer (e.g., Ref. 1) and is used here to derive metal temperature solutions for cases in which the water temperature versus time is more complex.

For $\phi(\tau) = 1$ (a unit step increase in water temperature at time = zero) the solution is

$$v(\xi,\tau) = F(\xi,\tau) = 1 - \sum_n A_n \cos[\alpha_n(1-\xi)]e^{-\alpha_n^2\tau} , \qquad (12)$$

where the parameters n are sequential integers from 1 to infinity and the parameters α_n are solutions to the transendental equation

$$\alpha_n \tan \alpha_n = \frac{h\ell}{k} = C \qquad (13)$$

and

$$A_n = \frac{2 \sin \alpha_n}{\alpha_n + \sin \alpha_n \cos \alpha_n} \qquad (14)$$

with

$$\sum_n A_n \cos[\alpha_n(1-\xi)] = 1 \quad \text{for} \quad 0 \le \xi \le 1 \quad . \qquad (15)$$

The first six roots, α_n, of $\alpha_n \tan \alpha_n = C$ for the selected values of C used in VISA are tabulated in Table A.1 which is taken from Reference 1. One may also note that for C = infinity and n = 1, 2, 3, ...

$$\alpha_n = (2n - 1)\frac{\pi}{2}$$

$$A_n = \frac{-(-1)^n}{(2n-1)} \cdot \frac{4}{\pi} \quad .$$

It can be shown that Equation (12) satisfies Equations (7) and (8) by taking the appropriate partial derivatives. Equation (13) results from Equation (9) and Equation (15) results from Equation (11). Equation (14) can be derived from Equation (15) as follows. To satisfy the initial condition for a unit step change in temperature,

$$\sum_n A_n \cos[\alpha_n(1-\xi)] = 1 \quad ,$$

one can multiply both sides by $\cos[\alpha_m(1-\xi)]d\xi$ and integrate 0 to 1. For $\alpha_m \neq \alpha_n$

TABLE A.1. The Roots of the Transcendental Equation $\alpha \tan \alpha = C$

C	α_1	α_2	α_3	α_4	α_5	α_6
6.0	1.3496	4.1116	6.9924	9.9667	12.9988	16.0654
10.0	1.4289	4.3058	7.2281	10.2003	13.2142	16.2594
20.0	1.4961	4.4915	7.4954	10.5117	13.5420	16.5864
40.0	1.5325	4.5979	7.6647	10.7334	13.8048	16.8794
60.0	1.5451	4.6353	7.7259	10.8172	13.9094	17.0026

$$\int_0^1 \cos[\alpha_m(1-\xi)]\cos[\alpha_n(1-\xi)]d\xi = \frac{1}{2}\left\{\frac{\sin(\alpha_m-\alpha_n)}{(\alpha_m-\alpha_n)} + \frac{\sin(\alpha_m+\alpha_n)}{(\alpha_m+\alpha_n)}\right\}$$

$$= \frac{\cos\alpha_m \cos\alpha_n}{[(\alpha_m)^2 - (\alpha_n)^2]}\left\{\alpha_m \tan\alpha_m - \alpha_n \tan\alpha_n\right\}$$

The righthand side equals zero, since for a given value of C, $\alpha_m \tan \alpha_m$ equals $\alpha_n \tan \alpha_n$. In general, however, $\alpha_m \neq \alpha_n$ when $m \neq n$. For $m = n$, one can show that

$$A_n \int_0^1 \cos^2[\alpha_n(1-\xi)]d\xi = \int_0^1 \cos[\alpha_n(1-\xi)]d\xi \quad ,$$

$$A_n \frac{\alpha_n + \sin\alpha_n \cos\alpha_n}{2\alpha_n} = \frac{\sin\alpha_n}{\alpha_n}$$

Solving for A_n, one obtains

$$A_n = \frac{2\sin\alpha_n}{\alpha_n + \sin\alpha_n \cos\alpha_n}$$

as given in Equation (14).

General Case of Water Temperature

A sketch of temperature variation in a vessel wall is shown in Figure A.1. Also illustrated are the various parameters in the above equations. The sketch indicates a water temperature decrease with time. For a heatup transient the temperature variation from T_0 would be inverted.

In this discussion $F(\xi,\tau)$, a special case of $v(\xi,\tau)$, is used to describe the temperature variation to avoid confusion in the analyses which follow.

Given that the solution for a unit step increase in water temperature at $\tau = 0$ is $F(\xi,\tau)$, then by Duhamel's Theorem (Ref. 1), the solution for a step increase of magnitude ϕ at $\tau = \lambda$ is $\phi \cdot F(\xi, \tau-\lambda)$. Similarly, the solution for a step decrease of ϕ at $\tau = \lambda + d\lambda$ is $-\phi \cdot F(\xi, \tau-\lambda-d\lambda)$.

Combining the above solutions, the solution for pulse of magnitude $\phi(\lambda)$ and width $d\lambda$ at $\tau = \lambda$ is

$$\phi(\lambda)[F(\xi, \tau-\lambda) - F(\xi, \tau-\lambda-d\lambda)] \quad ,$$

or

$$\phi(\lambda) \frac{\partial F}{\partial \tau} (\xi, \tau-\lambda)d\lambda$$

The general solution, $v(\xi,\tau)$, for a variable $\phi(\tau)$ can be derived from the special solution, $F(\xi,\tau)$, by

$$v(\xi,\tau) = \int_0^\tau \phi(\lambda) \frac{\partial}{\partial \tau} F(\xi, \tau-\lambda)d\lambda$$

$$= \sum_n \alpha_n^2 A_n \cos[\alpha_n(1-\xi)]e^{-\alpha_n^2\tau} \int_0^\tau \phi(\lambda)e^{\alpha_n^2\lambda} d\lambda \qquad (16)$$

where $\phi(\tau)$ is the water temperature variation from T_0 during the transient.

For most transients of interest, $\phi(\tau)$ will be a continuous function of τ. However, this is not a limitation of this procedure because if $\phi(\tau)$ is discontinuous, the integration can be performed from 0 to τ_f, and then from τ_f to τ where τ_f is the time at which $\phi(\tau)$ is discontinuous.

Integration of Equation (16) by parts provides a more generally useful solution for $v(\xi,\tau)$ in which the water temperature variation versus time is expressed as a separate term if $\phi(\tau)$ is single valued for all τ. Defining ϕ' as

$$\phi'(\tau) = d\phi/d\tau \text{ and } \sum_n A_n \cos[\alpha_n(1-\xi)] = 1 \quad ,$$

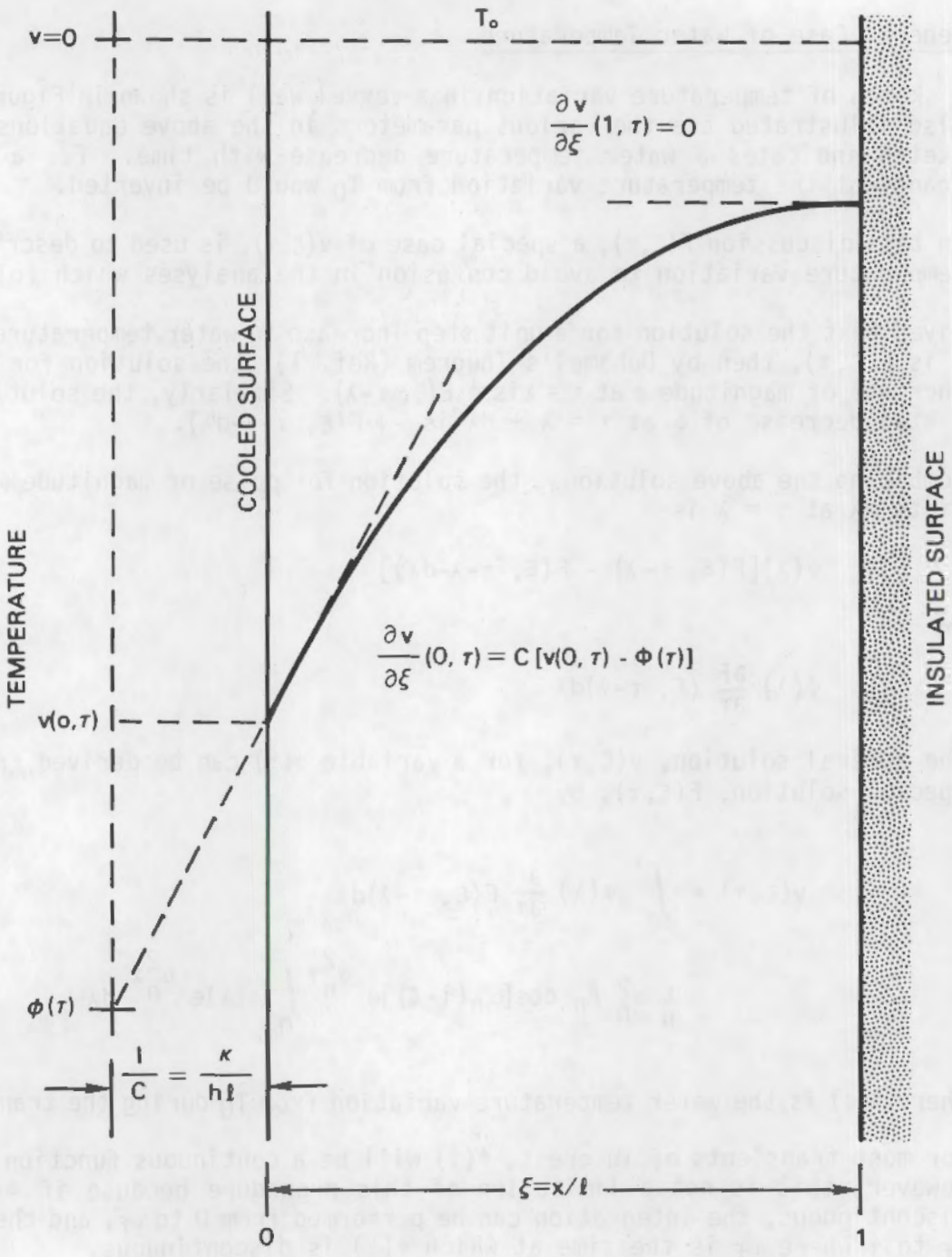

FIGURE A.1. General Case of Water Temperature Variation

$v(\xi,\tau)$ can then be expressed as

$$v(\xi,\tau) = \sum_n \alpha_n^2 A_n \cos[\alpha_n(1-\xi)]e^{-\alpha_n^2\tau}\left\{\left[\frac{\phi(\tau)e^{\alpha_n^2\tau}}{\alpha_n^2} - \frac{\phi(0)}{\alpha_n^2}\right] - \int_0^\tau \frac{\phi'(\lambda)e^{\alpha_n^2\lambda}d\lambda}{\alpha_n^2}\right\}$$

or

$$v(\xi,\tau) = \phi(\tau) - \sum_n A_n \cos[\alpha_n(1-\xi)]e^{-\alpha_n^2\tau}\left[\int_0^\tau \phi'(\lambda)e^{\alpha_n^2\lambda}\,d\lambda + \phi(0)\right] . \quad (17)$$

Again, care must be exercised in performing the integrations if $\phi'(\tau)$ is discontinuous at any time.

Specific examples of the temperature solution are given as follows.

(1) For a step change in water temperature of S_0 at $t = 0$, $\phi(\tau) = \phi(0) = S_0$, $\phi'(\tau) = 0$ and $v_0(\xi,\tau) = S_0F(\xi,\tau)$ as expected from Equation (12).

(2) For a ramp change in water temperature with $\phi(\tau) = \phi_1 t = [\phi_1(\ell^2/\kappa)]\tau = S_1\tau$, $\phi'(\tau) = S_1$, $\phi(0) = 0$ leads to:

$$v_1(\xi,\tau) = S_1\left\{\tau - \sum_n \frac{A_n}{\alpha_n^2}\cos[\alpha_n(1-\xi)]\left(1-e^{-\alpha_n^2\tau}\right)\right\} \quad (18)$$

(3) An alternate form of the ramp solution, Equation (18), can be obtained by a Taylor series expansion of $f_1(\xi) = \sum_n (A_n/\alpha_n^2)\cos[\alpha_n(1-\xi)]$ about $\xi = 1$ and, using $\sum_n A_n = 1$ from Equation (15) and $f'(0) = Cf_1(0)$ from Equation (9), it is found that

$$f_1(\xi) = \frac{1}{2}\left[\left(1 + \frac{2}{C}\right) - (1-\xi)^2\right]$$

and

$$v_1(\xi,\tau) = S_1\left\{\tau - \frac{1}{2}\left[\left(1 + \frac{2}{C}\right) - (1-\xi)^2\right] + \sum_n \frac{A_n}{\alpha_n^2}\cos[\alpha_n(1-\xi)]e^{-\alpha_n^2\tau}\right\} \quad (19)$$

which for large values of τ, approaches the parabolic temperature distribution often used to determine peak thermal stresses in a ramp cooldown transient.

(4) Defining,

$$B_n(\tau) = -A_n\, e^{-\alpha_n^2 \tau} \left[\int_0^{\tau} \phi'(\lambda) e^{\alpha_n^2 \lambda}\, d\lambda + \phi(0) \right] \tag{20}$$

where $B_n(\tau)$ depends on the specific transient being analyzed and

$$C_n(\xi) = \cos[\alpha_n (1 - \xi)] \tag{21}$$

Equation (17) becomes

$$v(\xi,\tau) = \phi(\tau) + \sum_n B_n(\tau)\, C_n(\xi) \tag{22}$$

or adding T_0 to each side,

$$T(\xi,\tau) = T_W(\tau) + \sum_n B_n(\tau)\, C_n(\xi) \tag{23}$$

It is important to note that in all the above examples, that $\tau (= \kappa t / \ell^2)$ is in fact a function of temperature. If κ varies significantly over the temperature range of interest, Equation (23) may have to be iterated a number of times to get consistent values of $T(\xi,t)$ and $\kappa(T)$. This is done by assuming an initial value for κ, calculating $T(\xi,t)$, determining a mean or effective value of κ for this T and redoing the calculation with this $\kappa(T)$. Consistent values of κ and T are usually obtained after 2 or 3 iterations. For most analyses, however, a constant value of κ can be selected to yield acceptable results. The thermal diffusivity $\kappa(T)$ and other parameters for a typical reactor vessel material are given below under the heading of material properties.

For later use in calculating thermal stresses and stress intensity factors, it is preferable to have $T(\xi,t)$ expressed as a polynomial in ξ for each time of interest. $T(\xi,t)$ is calculated at ξ = 0, 1/4, 1/2, 3/4, and 1 using Equation (23) and after iterating on κ, if desired, it is converted to

$$T(\xi,t) = A_0 + A_1\xi + A_2\xi^2 + A_3\xi^3 + A_4\xi^4 \tag{24}$$

using the curve fitting procedure described later in this appendix. It should be noted that the A's in Equation (24) are not the A_n's defined in Equation (14). The iteration on κ is performed for each of the five locations of the polynomial fit (ξ = 0, 1/4, etc.). In the converged solutions, the value of κ at the location of interest is assumed to be the appropriate value of constant κ which governs the heat transfer through the vessel wall.

Exponential Decay of Water Temperature

For many practical cases, the water temperature versus time can be fitted adequately by an expression

$$T_W(t) = T_0 + S(1 - e^{-\beta t}) \tag{25}$$

where S is a negative number and T_0, S, and β are determined by curve fitting.

The specific solution for this water temperature history, as shown in Figure A.2, can be obtained by defining

$$\omega^2 = \frac{\ell^2 \beta}{\kappa} \tag{26}$$

$$\phi(\tau) = S(1 - e^{-\omega^2 \tau}) \ , \quad \phi'(\tau) = S\omega^2 e^{-\omega^2 \tau} \ , \quad \phi(0) = 0$$

$$B_n(\tau) = - S A_n e^{-\alpha_n^2 \tau} \int_0^\tau \omega^2 e^{\left[\alpha_n^2 - \omega^2\right]\lambda} \, d\lambda$$

$$= \frac{SA_n}{\left[\left(\frac{\alpha_n}{\omega}\right)^2 - 1\right]} \left[e^{-\alpha_n^2 \tau} - e^{-\omega^2 \tau}\right] \tag{27}$$

Substituting Equations (25) and (27) into Equation (23), gives

$$T(\xi,\tau) = T_0 + S \left\{(1 - e^{-\omega^2 \tau}) + \sum_n \frac{A_n C_n(\xi)}{\left[\left(\frac{\alpha_n}{\omega}\right)^2 - 1\right]} \left[e^{-\alpha_n^2 \tau} - e^{-\omega^2 \tau}\right]\right\} \tag{28}$$

It can be noted that for ω^2 = infinity and S = S_0, Equation (28) becomes the solution for a step change in water temperature

$$T(\xi,\tau) = T_0 + S_0 \left\{1 + \sum_n A_n C_n(\xi) e^{-\alpha_n^2 \tau}\right\} = T_0 + S_0 F(\xi,\tau) \tag{29}$$

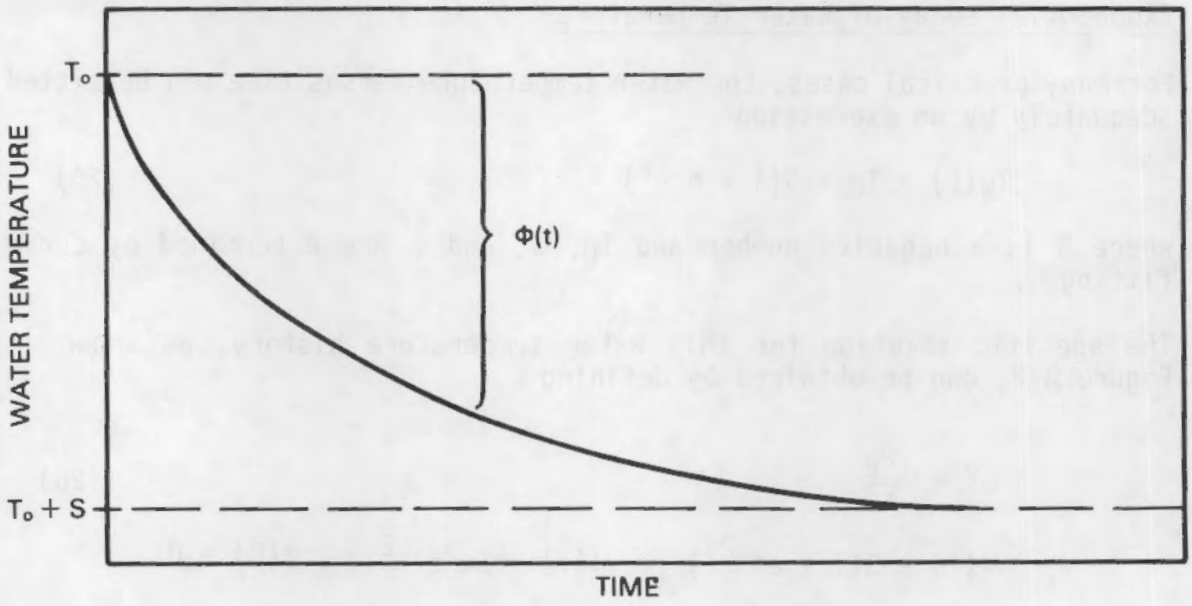

FIGURE A.2. Exponential Decay of Water Temperature

Also by specifying $S\omega^2$ = (a constant) = $(\phi, \ell^2/\kappa)$; that is, $S\beta = \phi_1$, where ϕ_1 is a ramp rate and then letting ω^2 approach zero, Equation (28) becomes the solution for a ramp change in water temperature.

$$T(\xi, \tau) = T_0 + S_1 \left[\tau - \sum_n \frac{A_n}{\alpha_n^2} C_n(\xi) \left(1 - e^{-\alpha_n^2 \tau}\right) \right] \qquad (30)$$

which is consistent with Equation (18).

Water Temperature Described by a Power Series Equation in Time

Assume that the water temperature can be expressed as a power series as shown in Figure A.3 for the time period of interest. The water temperature can then be described by

$$T_W = T_0 + \phi(t)$$

where

$$\phi(t) = \phi_0 + \phi_1 + \phi_2 t^2 + \ldots + \phi_m t^m \qquad (31)$$

and the ϕ_m are constants. Then the function ϕ takes on the form

$$\phi(\tau) = S_0 + S_1\tau + S_2\tau^2 + \ldots + S_m\tau^m \qquad (32)$$

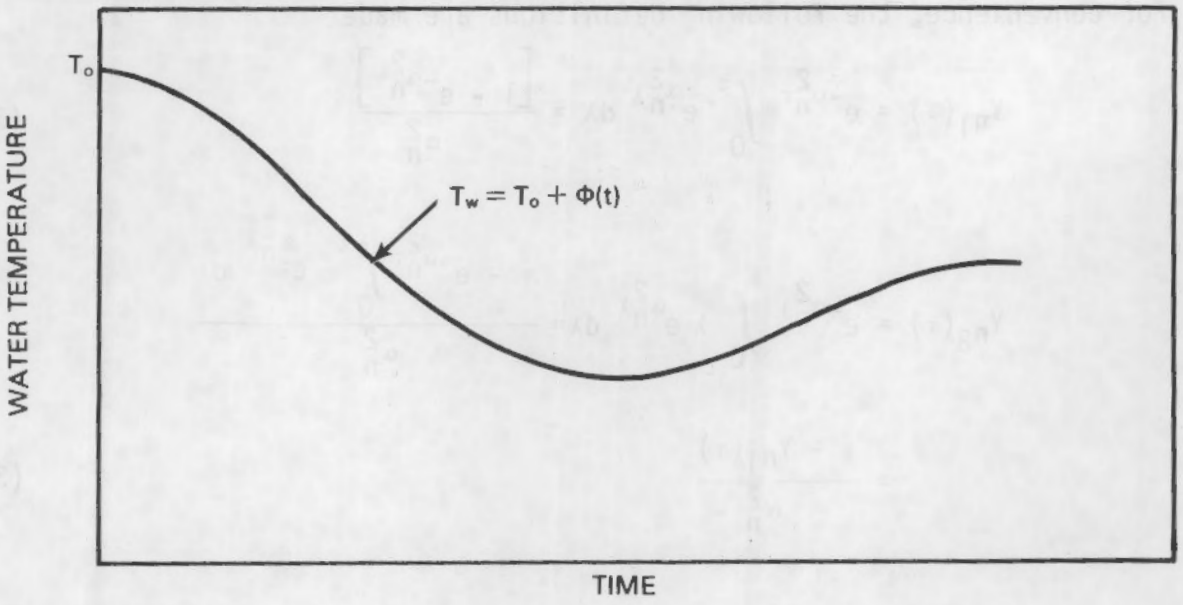

FIGURE A.3. Water Temperature Described by a Power Series Equation in Time

where

$$S_m = \phi_m \left(\frac{\ell^2}{\kappa}\right)^m \quad . \tag{33}$$

$T(\xi,\tau)$ will then be

$$T(\xi,\tau) = v_0(\xi,\tau) + v_1(\xi,\tau) + \ldots + v_m(\xi,\tau) \quad . \tag{34}$$

From Equation (32)

$$\phi'(\tau) = S_1 + 2S_2\tau + 3S_3\tau^2 + \ldots mS_m\tau^{m-1} \quad . \tag{35}$$

Substituting Equation (35) into Equation (20) with $\phi(0) = S_0 = \phi_0$ gives

$$B_n(\tau) = -A_n e^{-\alpha_n^2\tau}\left[S_0 + S_1\int_0^\tau e^{\alpha_n^2\lambda}\,d\lambda + 2S_2\int_0^\tau \lambda e^{\alpha_n^2\lambda}\,d\lambda\right.$$

$$\left. + 3S_3\int_0^\tau \lambda^2 e^{\alpha_n^2\lambda}\,d\lambda + \ldots + mS_m\int_0^\tau \lambda^{m-1} e^{\alpha_n^2\lambda}\,d\lambda\right]$$

For convenience, the following definitions are made

$$Y_{n_1}(\tau) = e^{-\alpha_n^2\tau} \int_0^\tau e^{\alpha_n^2\lambda}\, d\lambda = \frac{\left[1 - e^{-\alpha_n^2\tau}\right]}{\alpha_n^2} \tag{36}$$

$$Y_{n_2}(\tau) = e^{-\alpha_n^2\tau} \int_0^\tau \lambda\, e^{\alpha_n^2\lambda}\, d\lambda = \frac{\tau - e^{-\alpha_n^2\tau}\int_0^\tau e^{\alpha_n^2\lambda}\, d\lambda}{\alpha_n^2}$$

$$= \frac{\tau - Y_{n_1}(\tau)}{\alpha_n^2} \tag{37}$$

$$Y_{n_3}(\tau) = e^{-\alpha_n^2\tau}\int_0^\tau \lambda^2\, e^{\alpha_n^2\lambda}\, d\lambda = \frac{\tau^2 - 2e^{-\alpha_n^2\tau}\int_0^\tau \lambda e^{\alpha_n^2\lambda}\, d\lambda}{\alpha_n^2}$$

$$= \frac{\tau^2 - 2Y_{n_2}(\tau)}{\alpha_n^2} \tag{38}$$

$$Y_{n_m}(\tau) = e^{-\alpha_n^2\tau}\int_0^\tau \lambda^{m-1}\, e^{\alpha_n^2\lambda}\, d\lambda = \frac{\tau^{m-1} - (m-1)Y_{n_{(m-1)}}(\tau)}{\alpha_n^2} \tag{.30}$$

Then

$$B_n(\tau) = -A_n\left[S_0\, e^{-\alpha_n^2\tau} + S_1 Y_{n_1}(\tau) + 2S_2 Y_{n_2}(\tau)\right.$$

$$\left. + 3S_3 Y_{n_3}(\tau) + \ldots + mS_m Y_{n_m}(\tau)\right] \tag{40}$$

For most transients of interest, $S_0 = 0$ and the transients can be adequately described by 4 terms, S_1 to S_4 or ϕ_1 to ϕ_4. To obtain the constants, ϕ_m, the total transient time of interest can be divided into 4 equal increments and the water temperature at each of these times can be determined empirically from a plot of water temperature versus time. One can subtract T_0 from each of these temperatures and use the curve fitting procedure described below to get the ϕ_m's.

If ϕ_0 is not zero and

$$T_W(t) = T_0 + \phi_0 + \phi_1 t + \phi_2 t^2 + \phi_3 t^3 + \phi_4 t^4$$

$$= T_0 + S_0 + S_1\tau + S_2\tau^2 + S_3\tau^3 + S_4\tau^4 \qquad (41)$$

then

$$T(\xi,\tau) = T_W(\tau) - \sum_n A_n C_n(\xi) \left[S_0 e^{-\alpha_n^2 \tau} + S_1 Y_{n_1}(\tau) \right.$$

$$\left. + 2S_2 Y_{n_2}(\tau) + 3S_3 Y_{n_3}(\tau) + 4S_4 Y_{n_4}(\tau) \right] \qquad (42)$$

Note that the terms involving S_0 in Equation (42) represent the step solution if all other $S_m = 0$. Similarly, the terms involving S_1 represent the ramp solution if all other $S_m = 0$.

THERMAL STRESS DISTRIBUTIONS

This section describes the Equations used to calculate thermal stresses in the vessel wall, and also the Equations used to calculate the associated crack tip stress intensity factors due to thermal stress. In all these calculations, linear elastic behavior is assumed. For the thermal stress distributions a flat slab approximation is made, as was the case for the temperature distribution. However, for the stress intensity factors, influence functions for the actual cylindrical geometry of the vessel are utilized.

Stress Calculation

It is assumed that Equations such as those given above are available to calculate temperatures at any point in the wall of the vessel. Using such a solution it is assumed that $T(\xi,\tau)$ has been calculated at the specific locations $\xi = 0$, 1/4, 1/2, 3/4 and 1 for a particular transient and time of interest and that the parameter $[E\alpha/(1-\nu)]$ is known for each of these temperatures where

E = modulus of elasticity

α = linear coefficient of expansion

ν = Poisson's ratio.

Multiply each temperature by $[E\alpha/(1-\nu)]$ for that temperature to determine $[E\alpha/(1-\nu)]T$ at $\xi = 0, 1/4, 1/2, 3/4$ and 1. Using the curve fitting procedure described below, determine

$$\left(\frac{E\alpha}{1-\nu}\right)T = A_0 + A_1\xi + A_2\xi^2 + A_3\xi^2 + A_4\xi^4 \quad , \tag{43}$$

where the A's in this case are not the same as the A's previously used. The average value of $[E\alpha/(1-\nu)]T = \overline{[E\alpha/(1-\nu)]T}$ is then

$$\overline{\left(\frac{E\alpha}{1-\nu}\right)T} = A_0 + \frac{A_1}{2} + \frac{A_2}{3} + \frac{A_3}{4} + \frac{A_4}{5} \quad . \tag{44}$$

The thermal stress can then be expressed as

$$\sigma(\xi,t) = \overline{\left(\frac{E\alpha}{1-\nu}\right)T} - \left(\frac{E\alpha}{1-\nu}\right)T = \sigma_0 + \sigma_1\xi + \sigma_2\xi^2 + \sigma_3\xi^3 + \sigma_4\xi^4$$

$$= \sum_j \sigma_j\xi^j \tag{45}$$

where the σ_j are to be recalculated for each time of interest and

$$\sigma_0 = \left(\frac{A_1}{2} + \frac{A_2}{3} + \frac{A_3}{4} + \frac{A_4}{5}\right) \tag{46}$$

$$\sigma_1 = -A_1 \tag{47}$$

$$\sigma_2 = -A_2 \tag{48}$$

$$\sigma_3 = -A_3 \tag{49}$$

$$\sigma_4 = -A_4 \tag{50}$$

The above calculations can be done by computer assuming $[E\alpha/(1-\nu)]$ is expressed by:

$$\left(\frac{E\alpha}{1-\nu}\right) = e_0 + e_1T \quad e_2T^2 \tag{51}$$

over the temperature range of interest using the constants (e_0, e_1 and e_2) given below under the heading of material properties.

Fracture Mechanics Equations

For $\sigma(\xi,\tau)$ expressed as $\sum_j \sigma_j(\tau)\xi^j$, $\xi = x/\ell$, the procedure of Heliot et al. (Ref. 2) is used to determine $K_{I_T}(\alpha,\tau)$ where:

K_{I_T} = thermal component of the mode I stress intensity factor K_I

$\alpha = a/\ell$,

a = crack depth

ℓ = vessel wall thickness.

Then the crack tip stress intensity factor is given by

$$K_{I_T} = \sqrt{\pi a} \sum_j \sigma_j \alpha^j i_j$$

The i_j are polynomial influence functions. Equations for the i_j's for various crack geometries are as follows for $\alpha \leq 0.8$,

(1) Elliptical axial crack, a/c = 1/3, in a cylinder $R/\ell = 10$ for K_I at the deepest point of the crack ($\phi = 0^o$).

$$i_0 = 0.9000 + 0.3602\ \alpha + 0.2717\ \alpha^2$$
$$i_1 = 0.6087 - 0.0624\ \alpha + 0.3018\ \alpha^2$$
$$i_2 = 0.4844 - 0.1162\ \alpha + 0.2509\ \alpha^2$$
$$i_3 = 0.4048 - 0.1051\ \alpha + 0.1988\ \alpha^2$$
$$i_4 = 0.3602 - 0.1475\ \alpha + 0.2339\ \alpha^2$$

(2) Same geometry as in 1 above except for K_I at the surface, ($\phi = 90^o$).

$$i_0 = 0.5400 + 0.6675\ \alpha + 0.0250\ \alpha^2$$
$$i_1 = 0.0600 + 0.1246\ \alpha + 0.0708\ \alpha^2$$
$$i_2 = 0.0120 + 0.0913\ \alpha$$
$$i_3 = 0.0040 + 0.0525\ \alpha$$
$$i_4 = 0.0020 + 0.0338\ \alpha$$

(3) Long (infinite) axial crack in a cylinder, $R/\ell = 10$.

$$i_0 = 1.122 + 0.9513\,\alpha - 0.6240\,\alpha^2 + 8.3306\,\alpha^3$$
$$i_1 = 0.6825 + 0.3704\,\alpha - 0.0832\,\alpha^2 + 2.8251\,\alpha^3$$
$$i_2 = 0.5255 + 0.2011\,\alpha + 0.0313\,\alpha^2 + 1.4250\,\alpha^3$$
$$i_3 = 0.4414 + 0.1337\,\alpha + 0.0386\,\alpha^2 + 0.8806\,\alpha^3$$
$$i_4 = 0.3863 + 0.0989\,\alpha + 0.0437\,\alpha^2 + 0.5951\,\alpha^3$$

(4) Long circumferential crack in a cylinder, $R/\ell = 10$.

$$i_0 = 1.122 - 0.0100\,\alpha + 3.000\,\alpha^2$$
$$i_1 = 0.6825 - 0.0565\,\alpha + 1.2229\,\alpha^2$$
$$i_2 = 0.5255 - 0.1045\,\alpha + 0.7471\,\alpha^2$$
$$i_3 = 0.4414 - 0.1196\,\alpha + 0.5535\,\alpha^2$$
$$i_4 = 0.3863 - 0.0521\,\alpha + 0.3991\,\alpha^2$$

(5) Elliptical axial crack, $a/c = 1/10$, $R/\ell = 10$ for K_I at the deepest point of the crack.

$$i_0 = 1.0590 - 0.1619\,\alpha + 2.6930\,\alpha^2 - 0.9141\,\alpha^3$$
$$i_1 = 0.6590 - 0.1088\,\alpha + 1.1039\,\alpha^2 - 0.3955\,\alpha^3$$
$$i_2 = 0.5120 - 0.0164\,\alpha + 0.5491\,\alpha^2 - 0.1942\,\alpha^3$$
$$i_3 = 0.4470 - 0.0526\,\alpha + 0.4613\,\alpha^2 - 0.1986\,\alpha^3$$
$$i_4 = 0.3990 - 0.0056\,\alpha + 0.2566\,\alpha^2 - 0.0923\,\alpha^3$$

It should be emphasized that these influence functions can be used also for pressure and other stresses. For these cases, the stress must be written in the above polynomial form used for the thermal stresses.

The influence functions for the $a/c = 1/3$ and $1/10$ elliptical cracks (Cases 1, 2 and 5 above) are given here only for reference. The computer code VISA, as discussed in this report, treats only Cases and of the long axial and circumferential flaws. It should be noted that the surface lengths of the $a/c = 1/3$ and $1/10$ cracks are 6 and 20 times their respective depths.

The influence functions for Cases and correspond to those used in the version of the computer program VISA which is the subject of the present report, which was used for the NRC staff calculations reported in Ref. 3. Recent French work has resulted in some adjustments to these influence functions based on refined accuracy of numerical solutions. It is expected that future editions of VISA will use these more recent influence functions. For reference, the new influence functions are as follows.

(6) Elliptical axial crack, a/c = 1/3, in a cylinder R/ℓ = 10 for K_I at the deepest point of the crack ($\phi = 0^o$).

$$i_0 = 0.9200 + 0.1183\ \alpha + 0.9381\ \alpha^2 - 0.5255\ \alpha^3$$
$$i_1 = 0.6000 + 0.0104\ \alpha + 0.1097\ \alpha^2 + 0.1630\ \alpha^3$$
$$i_2 = 0.4620 + 0.0526\ \alpha - 0.1355\ \alpha^2 + 0.2767\ \alpha^3$$
$$i_3 = 0.3850 + 0.0426\ \alpha - 0.1316\ \alpha^2 + 0.2288\ \alpha^3$$
$$i_4 = 0.3200 + 0.1367\ \alpha - 0.3444\ \alpha^2 + 0.3418\ \alpha^3$$

(7) Long circumferential crack in a cylinder, R/ℓ = 10, $0 \leq \alpha \leq 0.8$.

$$i_0 = 1.122 + 0.3989\ \alpha + 1.5778\ \alpha^2 + 0.6049\ \alpha^3$$
$$i_1 = 0.6830 + 0.1150\ \alpha + 0.7556\ \alpha^2 + 0.1667\ \alpha^3$$
$$i_2 = 0.5260 + 0.1911\ \alpha - 0.1000\ \alpha^2 + 0.5802\ \alpha^3$$
$$i_3 = 0.4450 + 0.0783\ \alpha + 0.0556\ \alpha^2 + 0.3148\ \alpha^3$$
$$i_4 = 0.3880 + 0.1150\ \alpha - 0.1333\ \alpha^2 + 0.3519\ \alpha^3$$

Case (5) above for the a/c = 1/10 elliptical crack does not change since the influence functions as given already reflect the more recent French analyses.

PRESSURE STRESS DISTRIBUTIONS

The stresses due to internal pressure are computed using the equations for thick walled cylinders loaded by internal pressure. For circumferential stresses, the equation is

$$\frac{\sigma_\theta}{p} = \frac{r_i^2}{r_o^2 - r_i^2}\left(1 + \frac{r_o^2}{r^2}\right) \qquad (52)$$

where

p = internal pressure

r = radial coordinate

r_i = inside radius of vessel

r_o = outside radius of vessel.

In VISA, the cylinder dimensions are assumed always to give $r_o/r_i = 1.1$. For these particular vessel dimensions, one can fit a polynomial to the stresses predicted by Equation (5), and obtain

$$\frac{\sigma_\theta}{p} = 10.5238 - 1.1524\xi + 0.1727\,\xi^2 - 0.0225\,\xi^3 + 0.0022\,\xi^4 \qquad (53)$$

Using the influence functions given above for a long (infinite) axial crack in a cylinder with $r_o/r_i = 1.1$, one obtains the following result for the pressure induced stress intensity factor

$$\frac{K_{Ip}}{\sqrt{\ell}\,p} = \sqrt{\pi\alpha}\,\left[10.5238\, i_0(\alpha) - 1.1524\,\alpha\, i_1(\alpha) + 0.1727\,\alpha^2\, i_2(\alpha) - 0.0225\,\alpha^3\, i_3(\alpha) + 0.0022\,\alpha^4\, i_4(\alpha)\right] , \qquad (54)$$

where the i's are for the geometry number 3 of the above influence function discussion.

The axial stress in the vessel of dimensions $r_o/r_i = 1.1$ is uniform and is given by

$$\frac{\sigma_z}{p} = \text{constant} = 5.0$$

The corresponding stress intensity factor for a long (360 degree) circumferential crack is

$$\frac{K_{Ip}}{\sqrt{\ell}\ p} = 5\sqrt{\pi\alpha}\ [1.122 - 0.0100\ \alpha + 3.000\ \alpha^2] \quad . \qquad (55)$$

Figure A.4 shows plots of the solutions of Equations (54) and (55) for the stress intensity factors for axial and circumferential cracks. For shallow cracks, the axial crack has a stress intensity factor that is about twice that for a circumferential crack. As the cracks become deeper, this difference becomes significantly greater.

MATERIAL PROPERTIES

For the treatment of temperature dependent material properties, the VISA code has a specific set of properties. The user may choose to select these properties but should carefully compare these properties with the material properties for the vessel of interest. If the properties differ significantly, the user should provide input on the actual properties, rather than use the VISA default option. The user input properties will be treated as temperature independent. However, the effect of temperature dependence may be less important than the differences that may exist between the properties for the users grade of vessel steel and the default properties in VISA.

Figure A.5 shows plots of the temperature dependent properties that are used as a default option by VISA. These properties are consistent with properties for typical pressure vessel steels such as A533. The subroutines of VISA use the following equations

$$\frac{E\alpha}{1-\nu} = 0.285 + 1.351 \times 10^{-4}\ T - 9.465 \times 10^{-8}\ T^2 \qquad (56)$$

$$\kappa = 1.030 - 5.97 \times 10^{-7}\ T^2 \qquad (57)$$

$$k = 23.85\ [1 - 7.04 \times 10^{-7}\ (T-365)^2] \qquad (58)$$

where

E = elastic modulus, ksi

α = thermal expansion coefficient, $^{o}F^{-1}$

ν = Poisson's ratio (= 0.3 in VISA)

T = temperature, ^{o}F

κ = thermal diffusivity, $in.^{-2}/min$

k = thermal conductivity, Btu/hr·ft ^{o}F

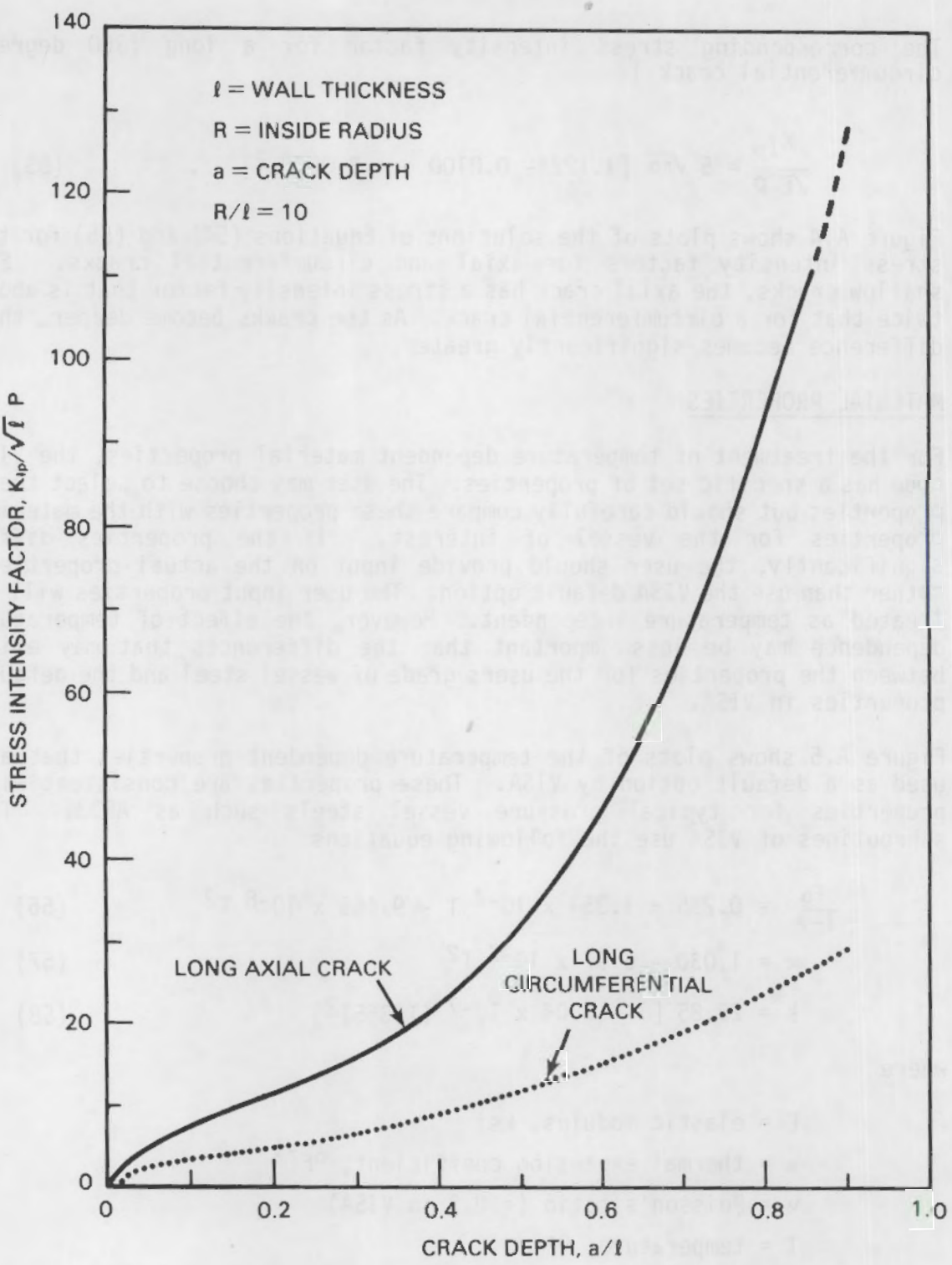

FIGURE A.4. Stress Intensity Factors for Internal Pressure

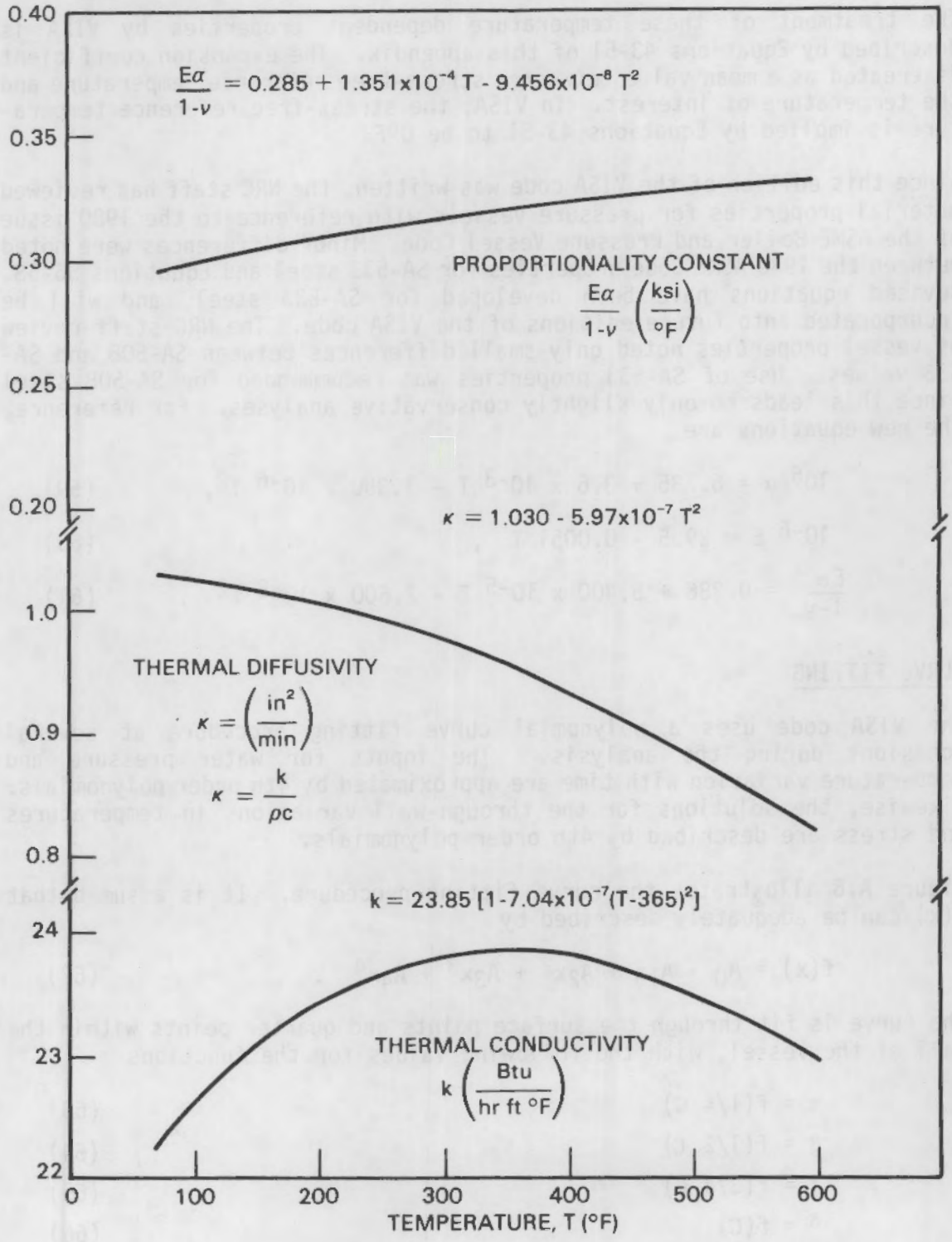

FIGURE A.5. Temperature Dependence of Material Properties

The treatment of these temperature dependent properties by VISA is described by Equations 43-51 of this appendix. The expansion coefficient is treated as a mean value between a stress-free reference temperature and the temperature of interest. In VISA, the stress-free reference temperature is implied by Equations 43-51 to be $0^{o}F$.

Since this edition of the VISA code was written, the NRC staff has reviewed material properties for pressure vessels with reference to the 1980 issue of the ASME Boiler and Pressure Vessel Code. Minor differences were noted between the 1980 ASME Code properties for SA-533 steel and Equations 56-58. Revised equations have been developed for SA-533 steel, and will be incorporated into future editions of the VISA code. The NRC staff review of vessel properties noted only small differences between SA-508 and SA-533 values. Use of SA-533 properties was recommended for SA-508 steel since this leads to only slightly conservative analyses. For reference, the new equations are

$$10^{6}\,\alpha = 6.785 + 3.6 \times 10^{-3}\,T - 1.350 \times 10^{-6}\,T^{2}, \qquad (59)$$

$$10^{-6}\,E = 29.5 - 0.0051\,T\ , \qquad (60)$$

$$\frac{E\alpha}{1-\nu} = 0.286 + 5.400 \times 10^{-5}\,T - 2.600 \times 10^{-8}\,T^{2}\ . \qquad (61)$$

CURVE FITTING

The VISA code uses a polynomial curve fitting procedure at several occasions during the analysis. The inputs for water pressure and temperature variation with time are approximated by 4th order polynomials. Likewise, the solutions for the through-wall variations in temperatures and stress are described by 4th order polynomials.

Figure A.6 illustrates the curve fitting procedure. It is assumed that f(x) can be adequately described by

$$f(x) = A_0 + A_1x + A_2x^2 + A_3x^3 + A_4x^4\ . \qquad (62)$$

The curve is fit through the surface points and quarter points within the wall of the vessel, with the following values for the functions

$$\alpha = f(1/4\ C) \qquad (63)$$

$$\beta = f(1/2\ C) \qquad (64)$$

$$\gamma = f(3/4\ C) \qquad (65)$$

$$\delta = f(C) \qquad (66)$$

$$f(0) = A_0$$

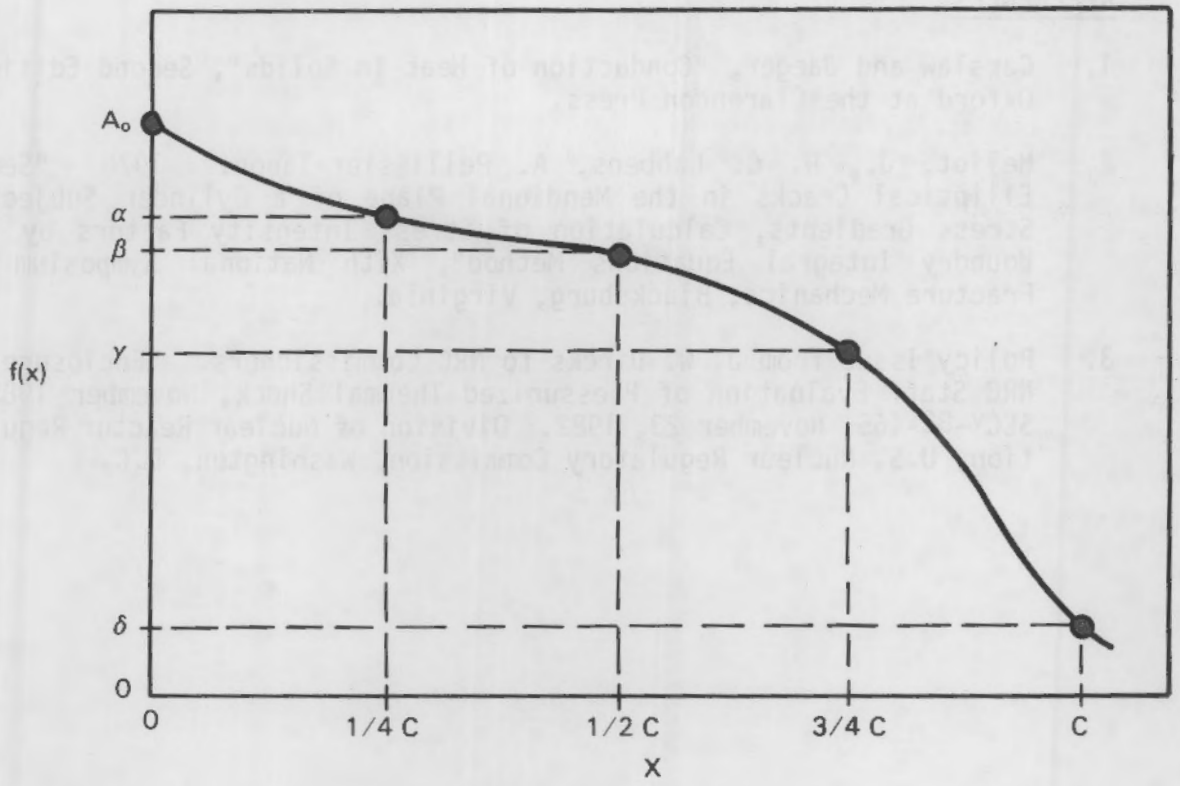

FIGURE A.6. Curve Fitting Procedure

Substituting in f(x) and solving for constants A

$$3A_1C = -25A_0 + 48\alpha - 36\beta + 16\gamma - 3\delta \quad (67)$$

$$\frac{3}{2} A_2C^2 = 35A_0 - 104\alpha + 114\beta - 56\gamma + 11\delta \quad (68)$$

$$\frac{3}{16} A_3C^3 = -5A_0 + 18\alpha - 24\beta + 14\gamma - 3\delta \quad (69)$$

$$\frac{3}{32} A_4C^4 = A_0 - 4\alpha + 6\beta - 4\gamma + \delta. \quad (70)$$

The average of the function f(x) over the interval x = 0 to C is given by

$$\bar{f} = \frac{1}{C} \int_0^C f\, dx = A_0 + \frac{A_1C}{2} + \frac{A_2C^2}{3} + \frac{A_3C^3}{4} + \frac{A_4C^4}{5}$$

$$= \frac{7}{90} A_0 + \frac{32}{90} \alpha + \frac{12}{90} \beta + \frac{32}{90} \gamma + \frac{7}{90} \delta \quad . \quad (71)$$

REFERENCES

1. Carslaw and Jaeger, "Conduction of Heat in Solids", Second Edition, Oxford at the Clarendon Press.

2. Heliot, J., R. C. Labbens, A. Pellissier-Tanon. 1978 "Semi-Elliptical Cracks in the Mendional Plane of a Cylinder Subjected Stress Gradients, Calculation of Stress Intensity Factors by the Boundry Integral Equations Method", XIth National Symposium on Fracture Mechanics, Blacksburg, Virginia.

3. Policy Issue from J. W. Dircks to NRC Commissioners. "Enclosure A: NRC Staff Evaluation of Pressurized Thermal Shock, November 1982." SECY-82-465, November 23, 1982. Division of Nuclear Reactor Regulation, U.S. Nuclear Regulatory Commission, Washington, D.C.

APPENDIX B

VALIDATION OF VISA HEAT TRANSFER, THERMAL STRESS AND STRESS INTENSITY ALGORITHMS

APPENDIX B

VALIDATION OF VISA HEAT TRANSFER, THERMAL STRESS AND STRESS INTENSITY ALGORITHMS

This appendix presents the results of a validation study of the heat transfer, thermal stress, and stress intensity algorithms in the VISA code. A typical PWR reactor geometry subjected to a postulated thermal transient was modeled with VISA and the results compared with similar solutions using the OCA-I (Ref. 1) and ANSYS (Ref. 2) codes. OCA-I was chosen for comparison because the code was written specifically to analyze pressure vessels that are subject to temperature and pressure transients and has been extensively applied in analysis of pressurized thermal shock. ANSYS was chosen because it is a widely used, well-documented, general-purpose finite element code.

The results from the three codes are shown in graphical form. Comparisons of the temperature and stress distributions through the vessel wall are shown for a given point in time during the transient. A comparison of the stress intensity values from the VISA and OCA-I codes is also given. Also presented here is a discussion of the exponential and polynomial representations that VISA uses for the reactor coolant temperature transient. Two transients are shown with their supposedly equivalent polynomial fits.

REACTOR VESSEL MODEL

The dimensions and material properties of a typical commercial PWR were used in the validation analyses. The major portion of these data was obtained from Table 2.1 of the OCA-I document. The report states that these are typical data for a PWR analysis. Table B.1 gives the pertinent data used in the validation analyses. The primary system pressure was taken as zero so that only the thermal transient contributes to the vessel-wall stresses.

The thermal transient used in the validation study is shown in Figure B.1. The figure represents exponential temperature decay from an initial temperature of 550°F to a final temperature of 250°F. The temperature at time, t, is given by the equation shown in Figure B.1. Here the decay constant, β, was taken as 0.15 for time measured in minutes. The first 96 minutes of the transient were analyzed in each of the three analyses.

The vessel model assumes that the wall of the carbon steel vessel has an inside radius of 86 inches and a wall thickness of 8.5 inches. In addition, the model includes a 0.25-inch-thick stainless steel cladding on the inside wall. This gives a true inside radius of 85.75 inches.

TABLE B.1. Vessel Data Used in VISA Validation

Carbon Steel/Vessel Data	
Inside Radius, inches	86
Outside Radius, inches	94.5
Wall Thickness, inches	8.5
Thermal Conductivity (k), Btu/hr·ft·°F	24
Specific Heat (C_p), Btu/lb·°F	0.12
Density (ρ), lb/ft^3	489
Stainless Steel Cladding Data	
Cladding Thickness (t), inches	0.25
Thermal Conductivity (k), Btu/hr·ft·°F	10.15
Initial Wall Temperature (T_o), °F	550
Primary-System Pressure, p ≠ f(t), psig	0
Convective Film Coefficient (h_c), Btu/hr·ft^2·°F	340

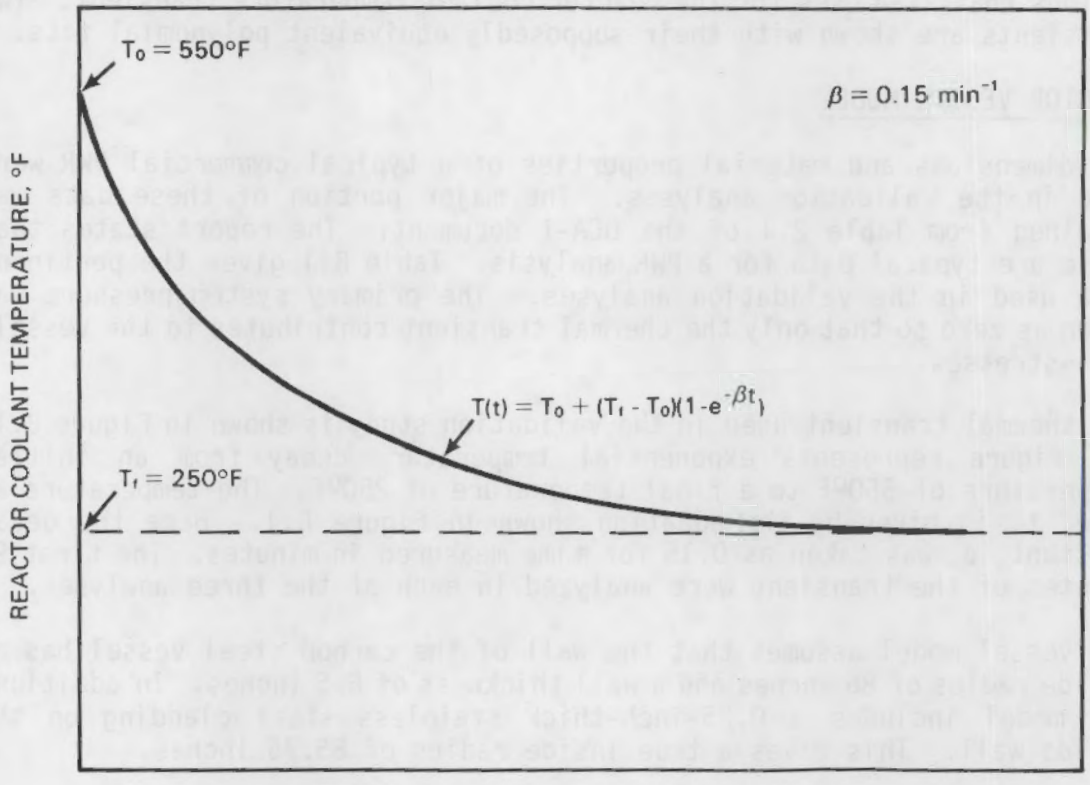

FIGURE B.1. Thermal Transient Used in Validation Models

Since OCA-I and VISA do not specifically treat cladding effects, modifications to the input data were required to ensure that the cladding was treated in an equivalent manner by each of the three codes. The ANSYS model used conduction links to model the thermal resistance of the cladding. OCA-I and VISA, on the other hand, do not consider the conduction through the cladding as a separate effect. Therefore, the heat transfer coefficient used in the VISA and OCA-I analyses must be an effective heat transfer coefficient which considers both convective heat transfer at the fluid-to-metal interface and conduction through the cladding. The calculation of the effective heat transfer coefficient, h_{eff}, is as follows:

$$h_{eff} = \frac{1}{\frac{1}{h_c} + \frac{t}{k}}$$

where

h_c = convective film coefficient

= 340 Btu/hr·ft^2·^{o}F

k = thermal conductivity of stainless steel

= 10.15 Btu/hr·ft·^{o}F

t = clad thickness = 0.25 inch

$$h_{eff} = \frac{1}{\frac{1}{340} + \frac{0.25\ (1/12)}{10.15}}$$

This calculation shows that the thermal effects of cladding are substantial and should be considered. The calculations show that for a 0.25-inch-thick stainless steel cladding, the convective film coefficient must be decreased by 40% if the effects of convection in the fluid and conduction through the cladding are combined.

No attempt was made to include the thermal stress effects of the cladding in the ANSYS model because similar effects are not treated in the VISA and OCA-I analyses. Therefore, graphical comparisons of the heat transfer solutions, thermal stresses, and stress intensity factor solutions only include the carbon steel portion of the vessel wall.

COMPARISON OF NUMERICAL RESULTS

Figure B.2 shows the temperature distributions through the vessel wall at 9.6 minutes into the transient for the VISA, OCA-I, and ANSYS heat transfer analyses. Data points in Figure B.2 from the three solutions are marked V, O, and A for VISA, OCA-I, and ANSYS, respectively. The figure shows close agreement between the temperature profiles of the three codes, thus supporting the validity of the VISA heat transfer analysis.

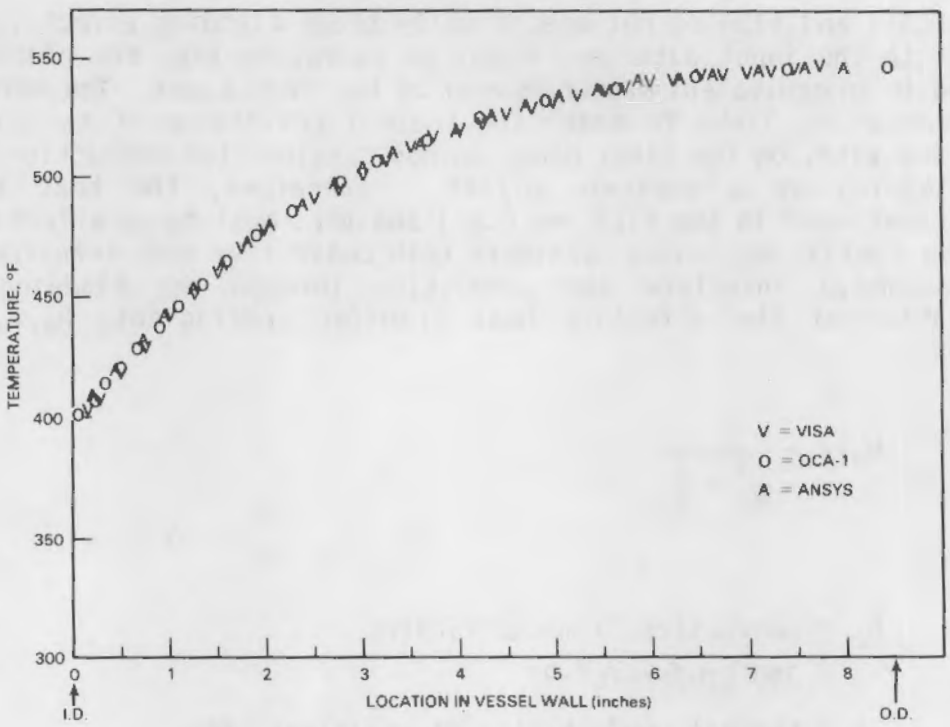

FIGURE B.2. Heat Transfer Solutions

Figure B.3 shows the circumferential thermal stresses which result from the through-wall temperature distributions of Figure B.2. The stress profiles in Figure B.3 are in close agreement, which supports the validity of the VISA thermal stress analysis.

Figure B.4 shows a comparison of the applied stress intensity factor values from the VISA and OCA-I analyses. The figure shows good agreement (within 5%) for flaws up to about three-quarters of the wall thickness, with VISA generally giving slightly higher values than OCA-I. Beyond three-quarters of the wall, the accuracy of the influence functions breaks down for both codes and the stress intensity factor values of Figure B.4 are of questionable validity.

VISA'S MODELING OF REACTOR COOLANT THERMAL TRANSIENTS

Within VISA the user has the option of specifying either an exponential or polynomial representation of the reactor coolant thermal transient. In using the exponential transient, the user specifies the initial and final temperatures and a decay constant, β. For the polynomial representation, the user specifies the initial and final temperatures as well as temperatures at quarter-point times during the transient. VISA then fits a polynomial through these temperatures.

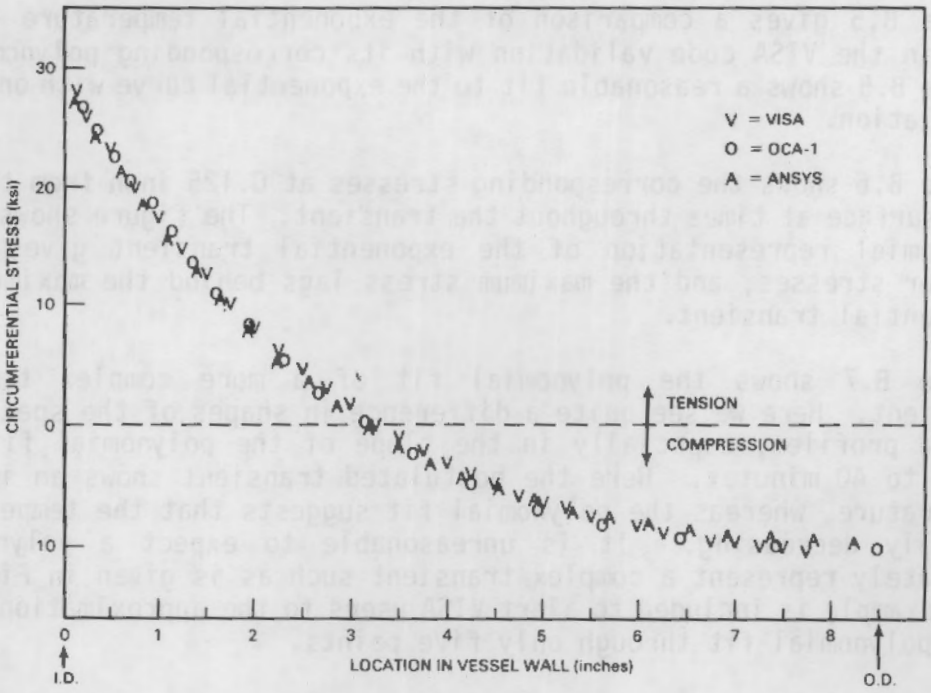

FIGURE B.3. Thermal Stress Solutions

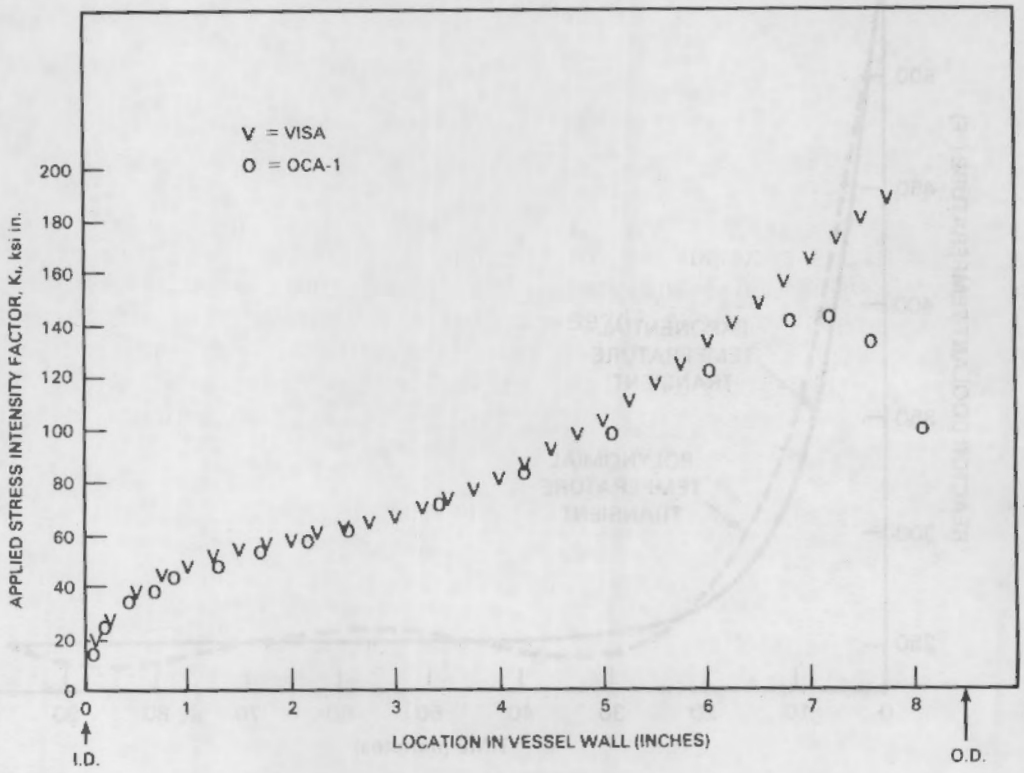

FIGURE B.4. Stress Intensity Factor Solutions

Figure B.5 gives a comparison of the exponential temperature transient used in the VISA code validation with its corresponding polynomial fit. Figure B.5 shows a reasonable fit to the exponential curve with only slight oscillation.

Figure B.6 shows the corresponding stresses at 0.125 inch from the inside wall surface at times throughout the transient. The figure shows that the polynomial representation of the exponential transient gives slightly smaller stresses, and the maximum stress lags behind the maximum of the exponential transient.

Figure B.7 shows the polynomial fit of a more complex temperature transient. Here we see quite a difference in shapes of the specified and fitted profiles, especially in the slope of the polynomial fit at time equal to 40 minutes. Here the postulated transient shows an increasing temperature, whereas the polynomial fit suggests that the temperature is actually decreasing. It is unreasonable to expect a polynomial to accurately represent a complex transient such as is given in Figure B.7. This example is included to alert VISA users to the approximations implied by a polynomial fit through only five points.

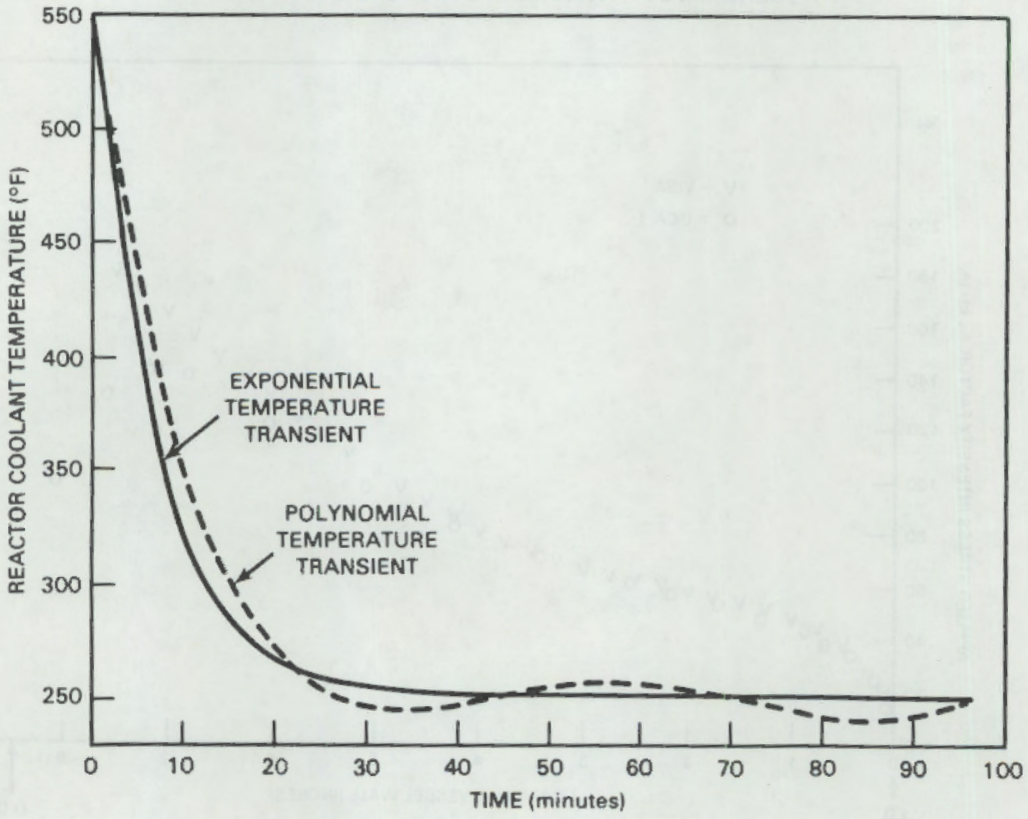

FIGURE B.5. Exponential and Polynomial Temperature Transients

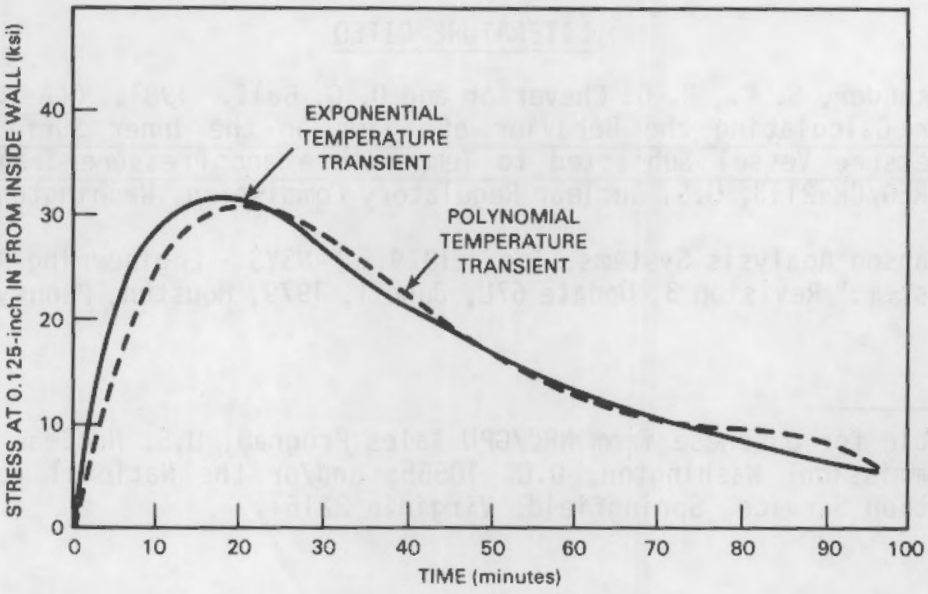

FIGURE B.6. Stresses Using Exponential and Polynomial Temperature Transients

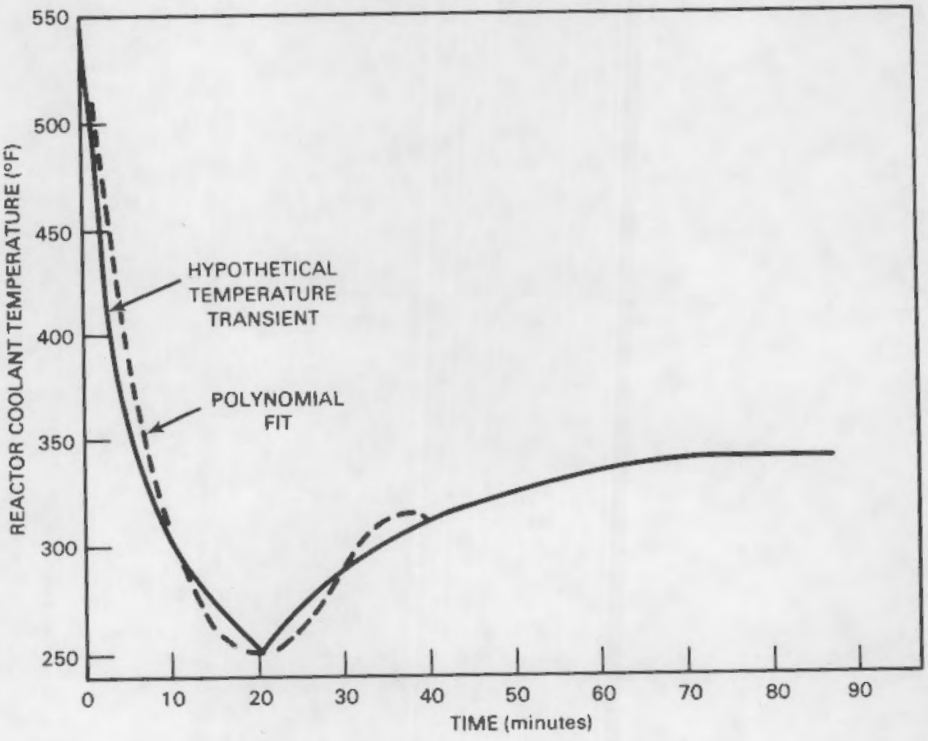

FIGURE B.7. Hypothetical and Polynomial Temperature Transients

LITERATURE CITED

1. Iskander, S. K., R. D. Cheverton and D. G. Ball. 1981. OCA-I, A Code for Calculating the Behavior of Flaws on the Inner Surface of a Pressure Vessel Subjected to Temperature and Pressure Transients. NUREG/CR-2113, U.S. Nuclear Regulatory Commission, Washington, D.C.*

2. Swanson Analysis Systems, Inc. 1979. "ANSYS - Engineering Analysis System." Revision 3, Update 67L, June 1, 1979, Houston, Pennsylvania.

*Available for purchase from NRC/GPO Sales Program, U.S. Nuclear Regulatory Commission, Washington, D.C. 10555; and/or the National Technical Information Service, Springfield, Virginia 22161.

APPENDIX C

RANDOM NUMBER GENERATION

APPENDIX C

RANDOM NUMBER GENERATION

The heart of any simulation program is the generation of random (actually pseudorandom) numbers. Random numbers are generated by an algorithm that produces a sequence of numbers between 0 and 1. Ideally, these numbers are uniformly distributed over the interval (0,1) with no statistical relationship between successive numbers.

Most large computer facilities have a random number generator available as part of the operating system, or resident in a library of mathematical subroutines. For the most part, these random number generator systems are adequate for generating small numbers of random numbers. However, a recent study (Ref. 1) has indicated that some generators in common use may not be adequate for large simulation studies. For this reason, a description of the most common algorithm is provided, and a suggestion is made for the selection of an adequate random number generator.

The most common way of producing pseudorandom numbers on a digital computer is to use the multiplicative congruential generator. A computationally efficient form of the algorithm produces a string of numbers z_1, z_2, z_3, ..., from the relationship

$$z_{i+1} = Az_i \text{ (modulo M)}$$

where A is called the multiplier of the generator and M is the modulus. The sequence begins with a value z_0 called the seed, which is supplied by the user.

The properties of the generator are determined by the constants selected for the multiplier A and the modulus M. To obtain the maximum number of random numbers before the sequence is repeated, the modulus should be taken as 2^p-1, where p is the computer word size in bits. The multiplier A largely controls the statistical properties of the generator, and also affects the relative execution time. Fishman and Moore (Ref. 1) tested 17 random number generators, using different values for A. The generator with A = 397204094 passed a battery of statistical tests with a relatively fast execution speed.

A multiplicative congruential random number generator is most efficiently coded using assembly language. The particular instructions are, therefore, machine dependent. The logical operations involved, however, are similar. Two sample listings are given below. One is for a computer with a 32-bit word. The other is for a 16-bit computer with a 32-bit arithmetic register. The code for the 16-bit computer will produce as many random numbers as would be available on a 32-bit machine.

```
        .TITLE RANF-RANDOM NUMBER GENERATOR
        .IDENT / V03/
        .GLOBL RANF
;
;         THIS SUBROUTINE GENERATES PSEUDO-RANDOM NUMBERS
;       USING THE MULTIPLICATIVE CONGRUENTIAL ALGORITHM
;
;       R(I+1) = A * R(I) * MOD(2**31 - 1)
;
;       WHERE
;               A    = MULTIPLIER = 397,204,094 (DECIMAL)
;                      A1 = UPPER 16 BITS = 013654 (OCTAL)
;                      A2 = LOWER 16 BITS = 155176 (OCTAL)
;               R(I) = OLD RANDOM NUMBER (SEED)
;
;               X * MOD(M) = X - INT(X/M) * M
;                   INT(Y) = INTEGER PART OF Y
;
;        THIS ROUTINE IS CALLED FROM VISA WITH THE STATEMENT
;
;               CALL RANF(I1,I2,R)
;
;       WHERE
;               I1 = UPPER 16 BITS OF THE SEED
;               I2 = LOWER 16 BITS OF THE SEED
;               R  = NEW RANDOM NUMBER
;
;         THIS ROUTINE WAS WRITTEN ON A PDP 11/70 (DEC),
;       USING THE PDP11 ASSEMBLER LANGUAGE.
;
;
;       GENERAL REGISTERS USED.
;
        R0=%0
        R1=%1
        R2=%2
        R3=%3
        R4=%4
        R5=%5
        SP=%6
        PC=%7
```

```
RANF:   TST     (R5)+           ; FINDS LOCATION OF I1.
;
;       A1 * I1
;
        MOV     @(R5),R2        ; MOVE I1 TO REG 2.
        MUL     A1,R2           ; A1 * I1.
;
;       A2 * I1
;
        MOV     A2,R0           ; MOVES A2 TO REG 0.
        ASR     R0              ; DIVIDE A2 BY 2.
        ROR     AODD            ; AODD NEGATIVE IF A2 ODD.
        BIC     #100000,R0      ; CLEAR BIT 31.
        MUL     @(R5),R0        ; MULT A2/2 BY I1.
        ASHC    #1,R0           ; MULT PRODUCT BY 2.
        TST     AODD            ; CHECK IF A2 IS ODD.
        BPL     A2I1            ; BRANCH IF EVEN.
        ADD     @(R5),R1        ; ADD I1 TO PRODUCT
        ADC     R0              ; ADD CARRY BIT.
        ADC     R2              ; ADD CARRY BIT.
A2I1:
        MOV     R1,R4           ; STORE BITS 17-31 IN R4.
        ADD     R0,R3           ; ADD TO BITS 32-47.
        ADC     R2              ; ADD CARRY BIT
;
;       A1 * I2
;
        MOV     @2(R5),R0       ; MOVE I2 TO R0
        ASR     R0              ; DIVIDE A2 BY 2.
        ROR     IODD            ; IODD NEGATIVE IF I2 ODD.
        BIC     #100000,RD      ; CLEAR BIT 31.
        MUL     A1,R0           ; MULT A1 BY I2/2.
        ASHC    #1,R0           ; MULT PRODUCT BY 2.
        TST     IODD            ; CHECK IF I2 IS ODD.
        BPL     A1I2            ; BRANCH IF EVEN
        ADD     A1,R1           ; ADD A1 TO PRODUCT.
        ADC     R0              ; ADD CARRY BIT.
        ADC     R2              ; ADD CARRY BIT.
A1I2:
        ADD     R1,R4           ; STORE BITS 17-31 IN R4.
        ADC     R0              ; ADD CARRY BIT
        ADC     R2              ; ADD CARRY BIT
        ADD     R0,R3           ; ADD TO BITS 32-47.
        ADC     R2              ; ADD CARRY BIT.
```

```
;
;       A2 * I2
;
        MOV     A2,R0           ; MOVES A2 TO REG 0.
        ASR     R0              ; DIVIDE A2 BY 2.
        BIC     #100000,R0      ; CLEAR BIT 16 OF REG 0.
        MOV     @2(R5),R1       ; MOVES I2 TO REG 1.
        ASR     R1              ; DIVIDE I2 BY 2.
        BIC     #100000,R1      ; CLEAR BIT 16 OF REG 1.
        MUL     R1,R0           ; A2/2 * I2/2.
        ASHC    #2,R0           ; SHIFT R0 & R1 2 TO THE LEFT.
        TST     A0DD            ; TESTING A2.
        BPL     TI2             ; BRANCH IF A2 EVEN.
        ADD     @2(R5),R1       ; I2 + A2/2 * I2/2.
        ADC     R0              ; ADD CARRY TO BITS 16-31.
TI2:    TST     I0DD            ; TESTING I2.
        BPL     XP              ; BRANCH IF I2 EVEN.
        ADD     A2,R1           ; A2 + A2/2 * I2/2.
        ADC     R0              ; ADD CARRY TO BITS 16-31.
        ADC     R3              ; ADD CARRY TO BITS 32-47.
        ADC     R2              ; ADD CARRY TO BITS 48-63.
        BIT     A0DD,I0DD       ; CHECK BOTH I2 AND A2 ODD.
        BPL     XP              ; BRANCH IF ONE EVEN.
        SUB     #1,R1           ; SUBTRACT 1 IF BOTH ODD.
        SBC     R0              ; SUBTRACT CARRY BIT.
        SBC     R3              ; SUBTRACT CARRY BIT
        SBC     R2              ; SUBTRACT CARRY BIT.
;
;       X'(N+1) = X(N+1) + R
;
XP:     ADD     R4,R0           ; GET BITS 16-31.
        ADC     R3              ; CARRY TO BITS 32-47.
        ADC     R2              ; CARRY TO BITS 48-63.
        ASHC    #1,R2           ; SHIFT R2 & R3 LEFT 1 BIT.
        ASL     R0              ; ISOLATE LOW-ORDER 31 BITS.
        ADC     R3              ; PUT BIT 32 INTO HIGH-ORDER.
        ASR     R0              ; REPLACE R0.
        BIC     #100000,R0      ; CLEAR BIT 32.
        ADD     R3,R1           ; ADD LOW-ORDER PARTS.
        ADC     R2              ; ADD CARRY INTO HIGH-ORDER.
        ADD     R2,R0           ; ADD HIGH-ORDER PARTS.
        BVS     OVF             ; BRANCH IF OVERFLOW (GT 2**31 - 1).
PLUS:   MOV     R0,@(R5)        ; RETURN NEW I1 VALUE.
        MOV     R1,@2(R5)       ; RETURN NEW I2 VALUE.
        MOV     #201,R2         ; INITIAL EXPONENT.
```

```
NORM:   ASL     R1              ; FLOAT RESULT.
        ROL     R0              ;
        BCS     EXP             ; JUMP IF LEADING BIT FOUND.
        DEC     R2              ; COMPENSATE EXPONENT.
        BR      NORM            ;
OVF:    BIC     #100000,R0      ; MAKES SURE R0 (NEW I1) IS POSITIVE.
        ADD     #1,R1           ; ADD 1 TO GET X'(N+1).
        ADC     R0              ; ADD CARRY BIT
        BR      PLUS            ; BRANCH TO PLUS TO RETURN VALUES.
EXP:    CLRB    R1              ;
        BISB    R0,R1           ;
        SWAB    R1              ;
        CLRB    R0              ;
        BISB    R2,R0           ; INSERT EXPONENT IN RESULT.
        SWAB    R0              ;
        ROR     R0              ;
        ROR     R1              ;
        MOV     4(R5),R3        ;
        MOV     R0,(R3)+        ; RETURNS RANDOM #.
        MOV     R1,(R3)+        ;
        RTS     PC              ;
AODD:   0                       ; WORK SPACE.
IODD:   0                       ; WORK SPACE.
A1:     013654                  ; UPPER 16 BITS OF MULTIPLIER.
A2:     155176                  ; LOWER 16 BITS OF MULTIPLIER.
        .END
```

LITERATURE CITED

1. Fishman, G. S. and L. R. Moore. 1982. "A Statistical Evaluation of Multiplicative Congruential Random Number Generators with Modulus $2^{31}-1$." J. Amer. Stat. Assoc. 77:129-136.

NUREG/CR-3384
PNL-4774
AM

DISTRIBUTION

No. of Copies

OFFSITE

200 U.S. Nuclear Regulatory Commission
Division of Technical Information
and Document Control
Washington, D.C. 20555

15 c/o J. Strosnider, Jr.
U.S. Nuclear Regulatory Commission
Division of Engineering Technology/RES
Materials Engineering Branch
Washington, D.C. 20555

15 c/o R. W. Klecker
U.S. Nuclear Regulatory Commission
Division of Engineering Technology/RES
Materials Engineering Branch
Washington, D.C. 20555

No. of Copies

50 Pacific Northwest Laboratory

W. J. Apley
M. C. Bampton
C. A. Bennett (HARC)
S. H. Bian
S. H. Bush
S. H. Dahlgren
D. W. Engel
C. R. Hann
A. J. Haverfield
K. I. Johnson
W. W. Laity
J. A. Mahaffey
R. P. Marshall
C. M. Novich
L. T. Pedersen (10)
P. J. Pelto
G. J. Posakony
R. E. Rhoads
E. P. Simonen
F. A. Simonen (5)
D. L. Stevens (5)
A. M. Sutey
T. T. Taylor
D. S. Trent
R. D. Widrig
L. D. Williams
Publishing Coordination (2)
Technical Information (5)

NRC FORM 335 (11-81)

U.S. NUCLEAR REGULATORY COMMISSION

BIBLIOGRAPHIC DATA SHEET

1. REPORT NUMBER (Assigned by DDC)
NUREG/CR-3384
PNL-4774

4. TITLE AND SUBTITLE (Add Volume No., if appropriate)
VISA - A Computer Code for Predicting the Probability of Reactor Pressure Vessel Failure

2. (Leave blank)

3. RECIPIENT'S ACCESSION NO.

7. AUTHOR(S)
D.L. Stevens, F.A. Simonen, J. Strosnider, Jr., R.W. Klecker, D.W. Engel, K.I. Johnson

5. DATE REPORT COMPLETED
MONTH: July YEAR: 1983

9. PERFORMING ORGANIZATION NAME AND MAILING ADDRESS (Include Zip Code)
Pacific Northwest Laboratory
Richland, Washington 99352

DATE REPORT ISSUED
MONTH: September YEAR: 1983

6. (Leave blank)

8. (Leave blank)

12. SPONSORING ORGANIZATION NAME AND MAILING ADDRESS (Include Zip Code)
Division of Engineering Technology
Office of Nuclear Regulatory Research
U.S. Nuclear Regulatory Commission
Washington, D.C. 20555

10. PROJECT/TASK/WORK UNIT NO.

11. FIN NO.
B-2310

13. TYPE OF REPORT
Technical

PERIOD COVERED (Inclusive dates)

15. SUPPLEMENTARY NOTES

14. (Leave blank)

16. ABSTRACT (200 words or less)

The VISA (Vessel Integrity Simulation Analysis) code was developed as part of the NRC staff evaluation of pressurized thermal shock. VISA uses Monte Carlo simulation to evaluate the failure probability of a pressurized water reactor (PWR) pressure vessel subjected to a pressure and thermal transient specified by the user. Linear elastic fracture mechanics are used to model crack initiation and propagation. Parameters for initial crack size, copper content, initial RT_{NDT}, fluence, crack-initiation fracture toughness, and arrest fracture toughness are treated as random variables. This report documents the version of VISA used in the NRC staff report (Policy Issue from J. W. Dircks to NRC Commissioners, "Enclosure A: NRC Staff Evaluation of Pressurized Thermal Shock, November 1982," SECY-82-465) and includes a user's guide for the code.

17. KEY WORDS AND DOCUMENT ANALYSIS

17a. DESCRIPTORS

17b. IDENTIFIERS/OPEN-ENDED TERMS

18. AVAILABILITY STATEMENT
Unlimited

19. SECURITY CLASS (This report)
unclassified

21. NO. OF PAGES

20. SECURITY CLASS (This page)
unclassified

22. PRICE
$

NRC FORM 335 (11-81)